



*The Waisman Laboratory
for Brain Imaging and Behavior*



University of Wisconsin
**SCHOOL OF MEDICINE
AND PUBLIC HEALTH**

Kernel Regression on Irregular Image Domains

Moo K. Chung

University of Wisconsin-Madison
www.stat.wisc.edu/~mchung

Abstract

We present the discrete version of heat kernel smoothing on graph data structure. The method is used to smooth data in an irregularly shaped domains in 3D images. New statistical properties of heat kernel smoothing are derived. As an application, we show how to filter out noisy data in the lung blood vessel trees obtained from computed tomography. The method can be further used in representing the complex vessel trees parametrically as a linear combination of basis functions and extracting the skeleton representation of the trees. This talk is based on [Chung et al. 2018. EMBC.](#)

Acknowledgement

Richard Davidson, Ruth Sullivan,
Michael Johnson, Michael Newton
University of Wisconsin-Madison

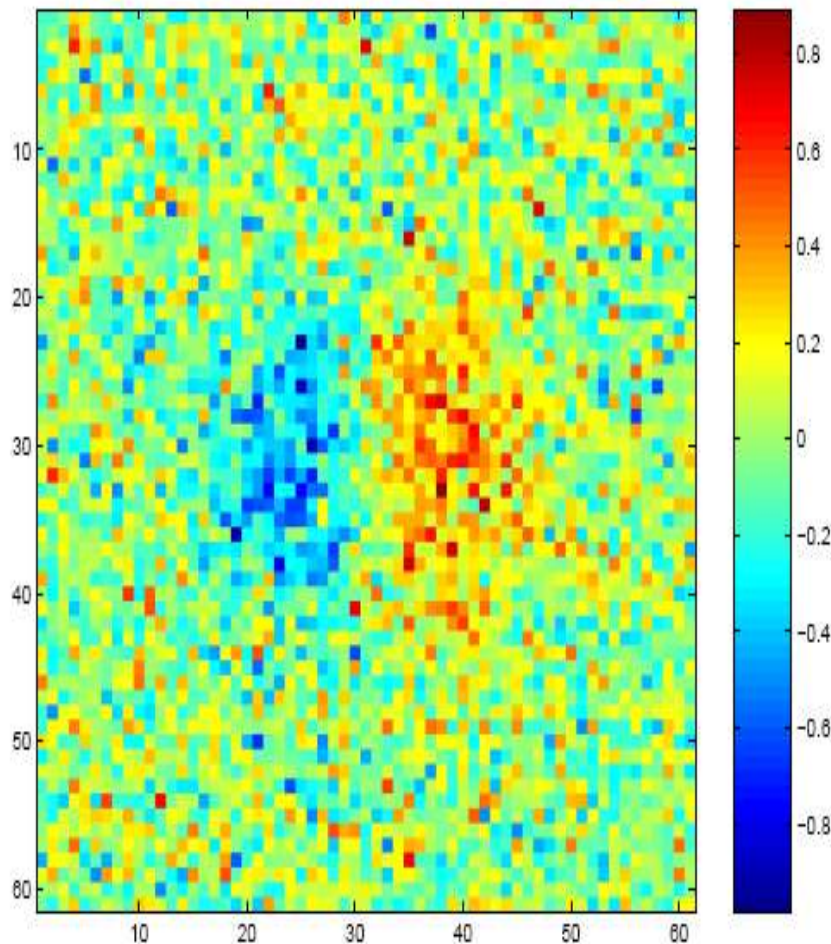
Gurong Wu
University of North Carolina-Chapel Hill

Yanli Wang
*Institute of Applied Physics and
Computational Mathematics, Beijing*

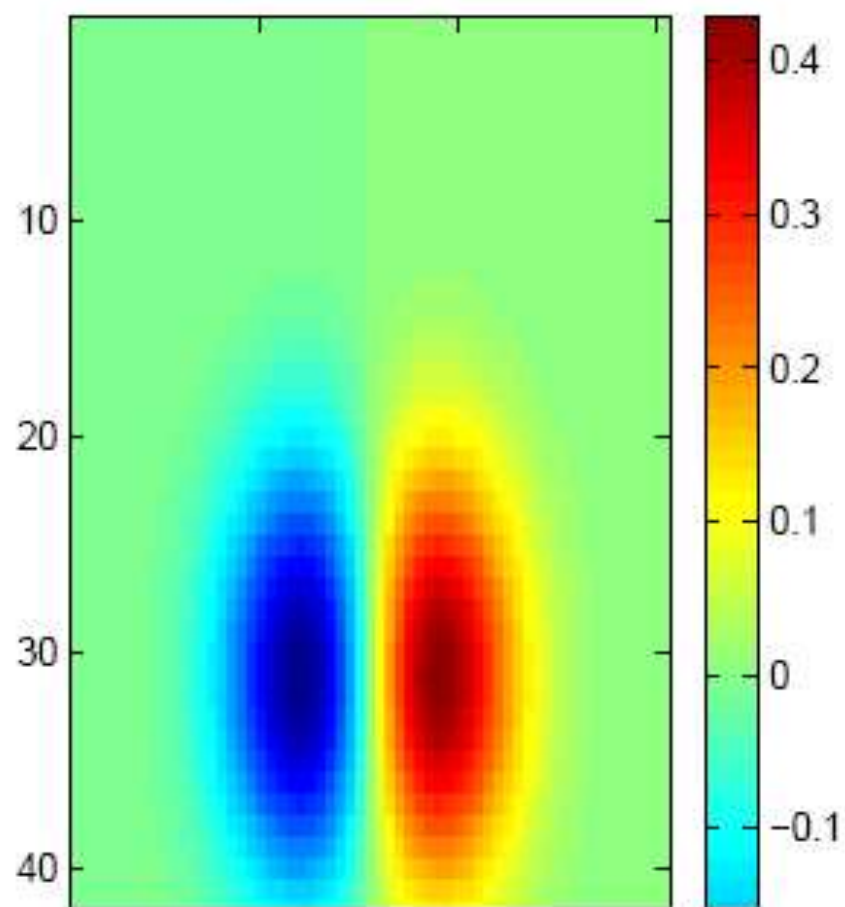
Gaussian kernel smoothing

$$Y(p) = \mu(p) + e(p)$$

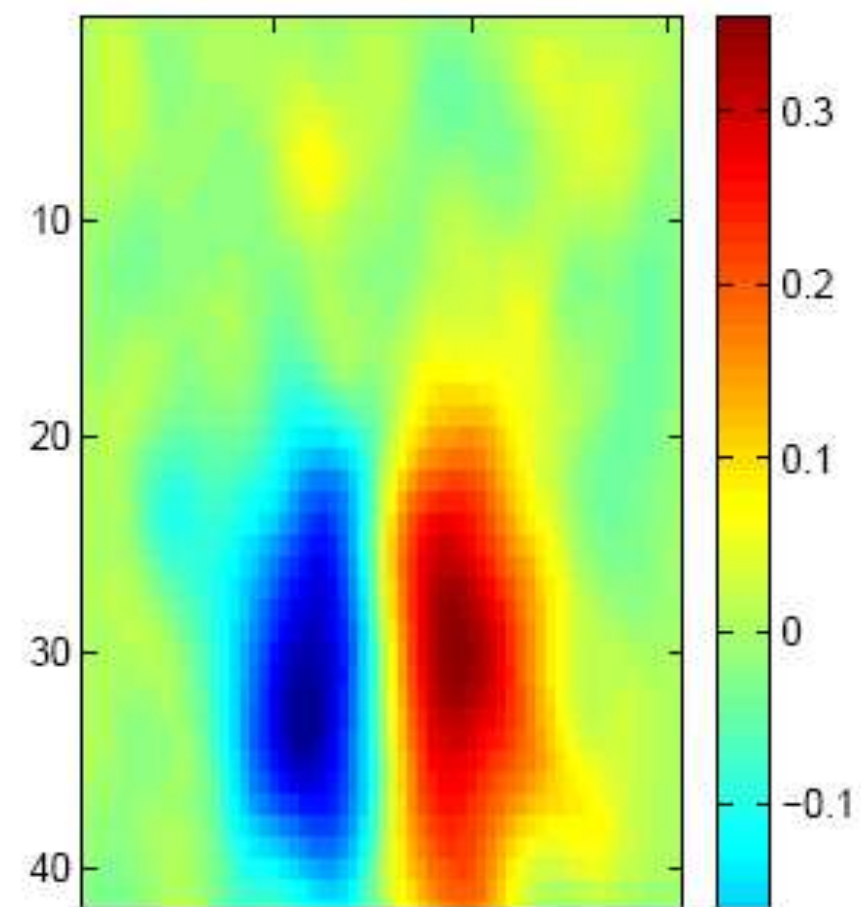
$$\hat{\mu}(p) = \int K(p, q) Y(p) dp$$



Observation $Y(p)$

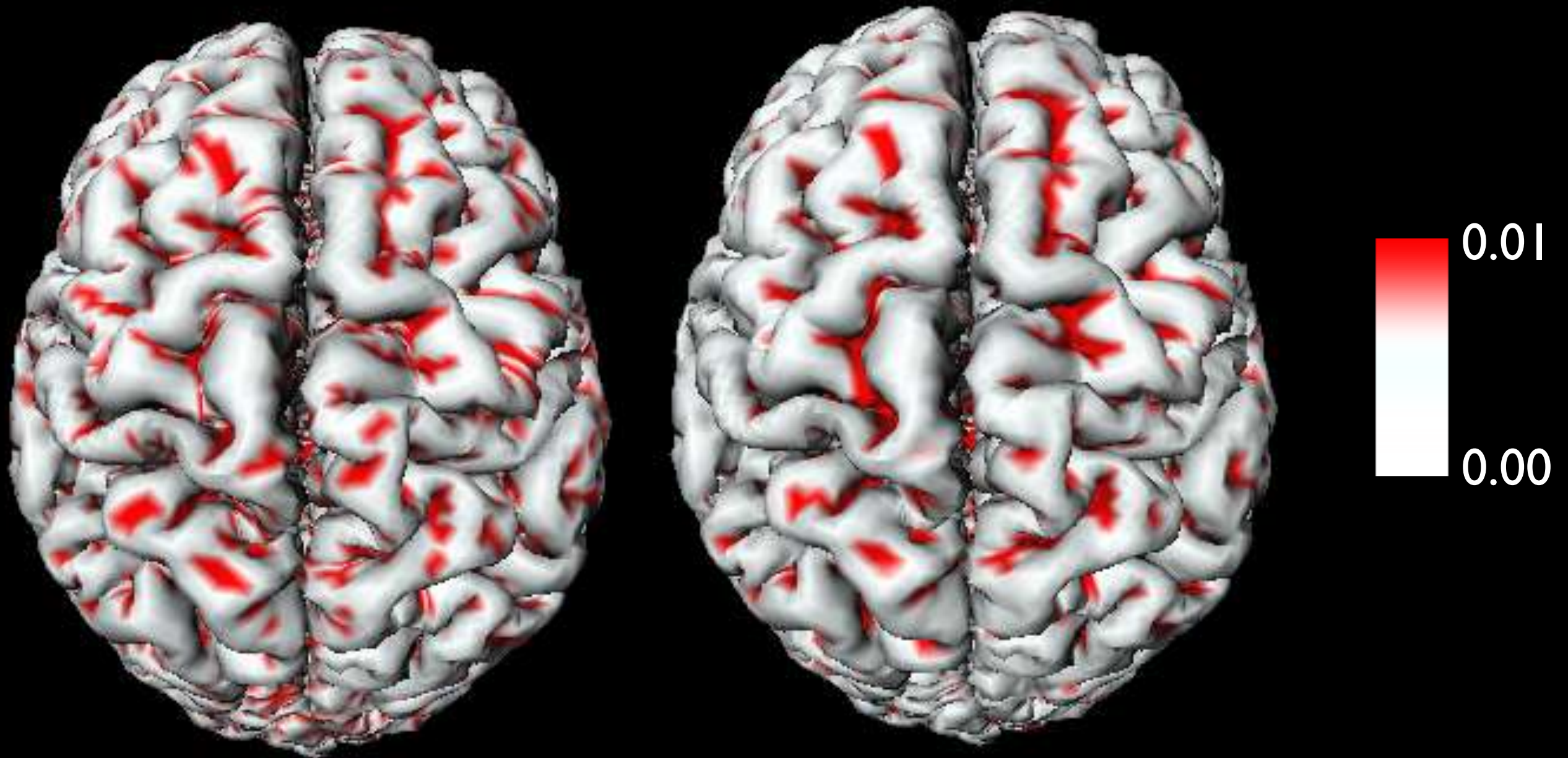


Unknown Signal $\mu(p)$



Prediction $\hat{\mu}(p)$

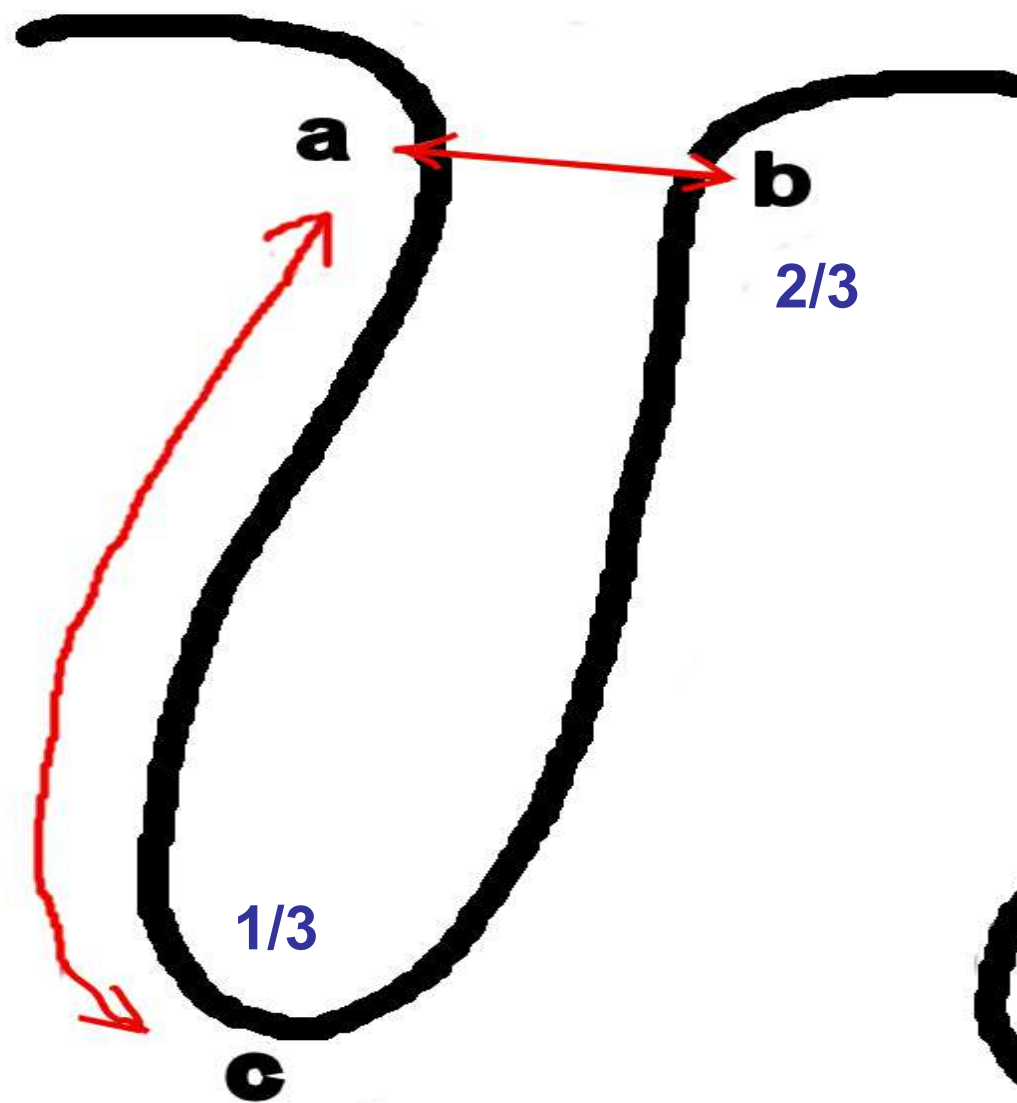
Gaussian kernel smoothing on surface curvature?



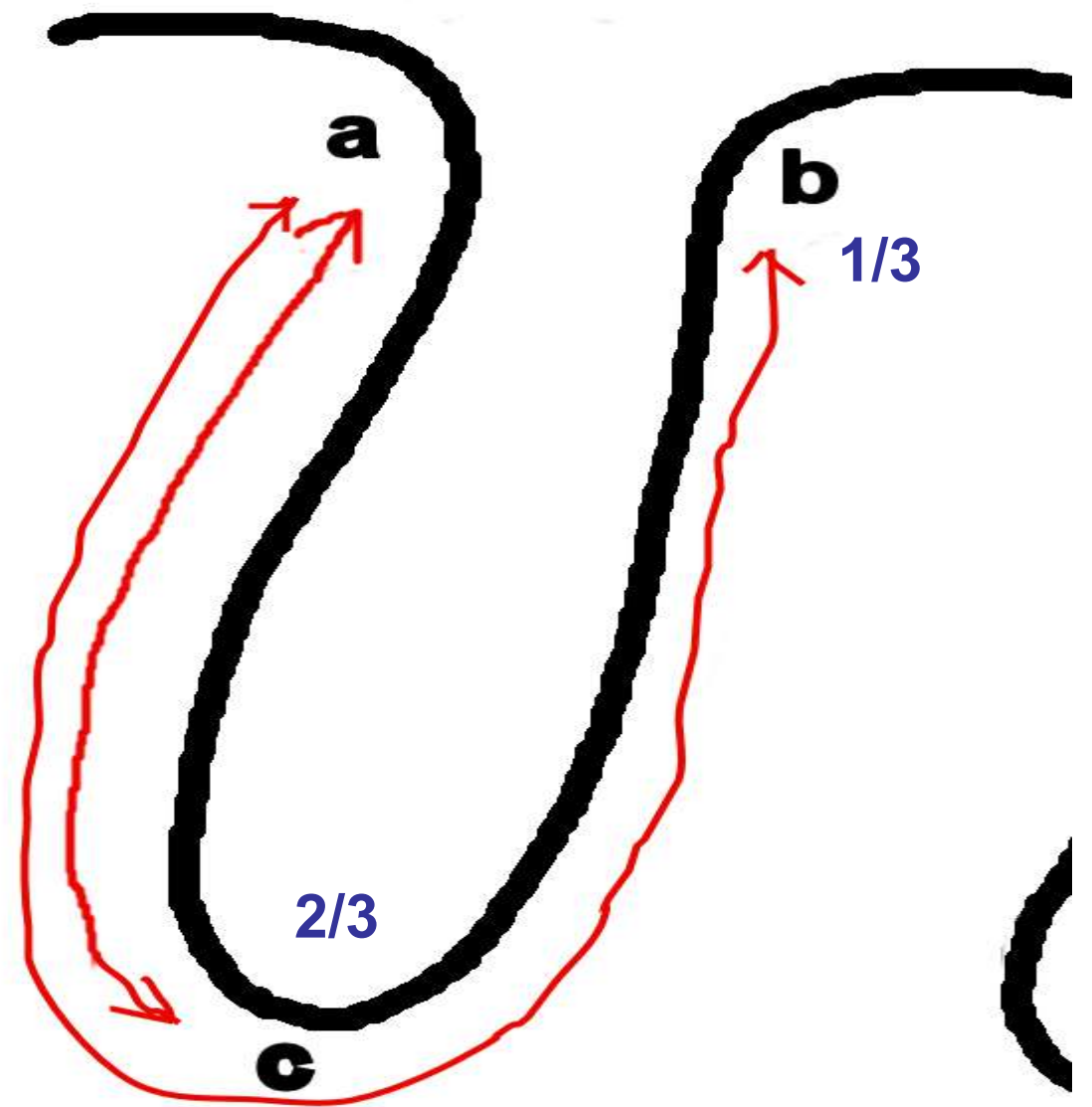
mean curvature

Noise removed curvature

Gaussian kernel does not work for surface data



Improper kernel weighting



Proper kernel weighting

Kernel smoothing on sphere

Magnetic Resonance Imaging (MRI)

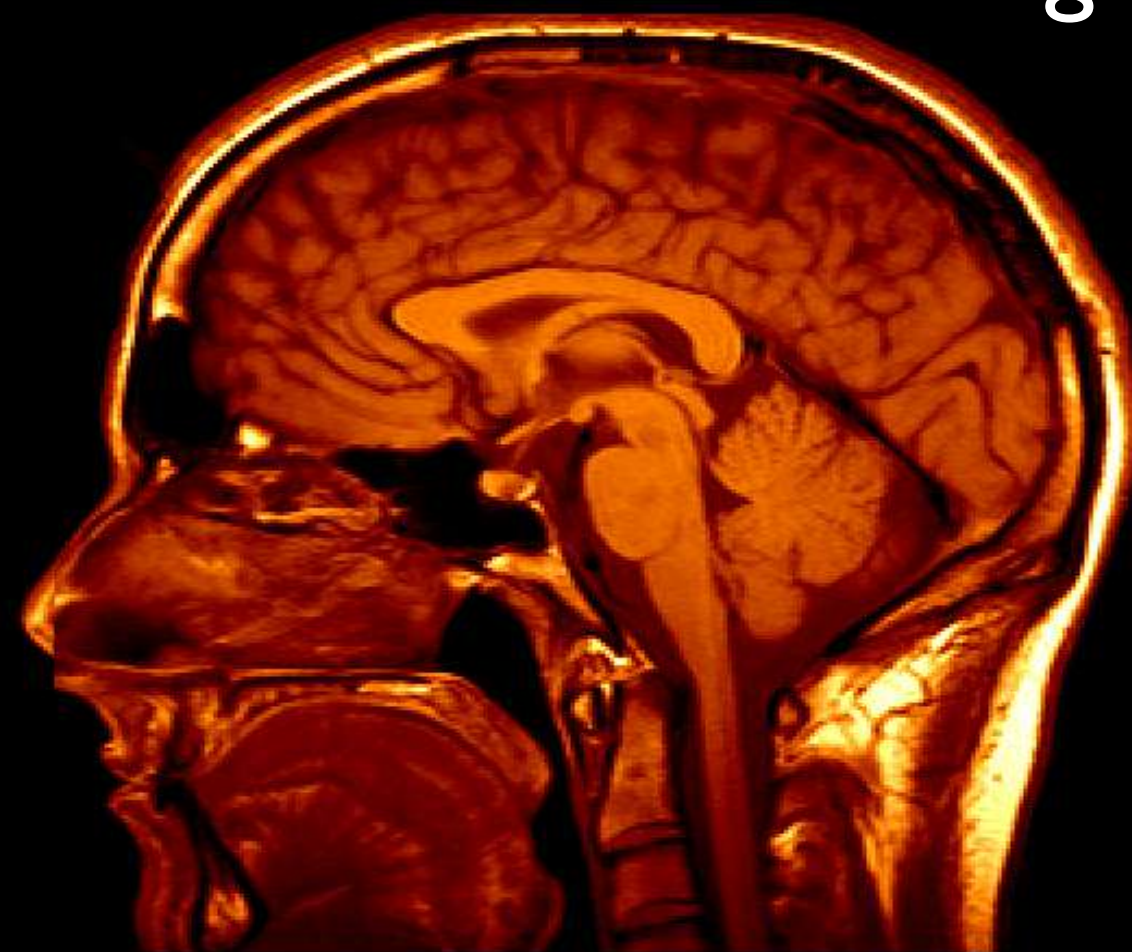


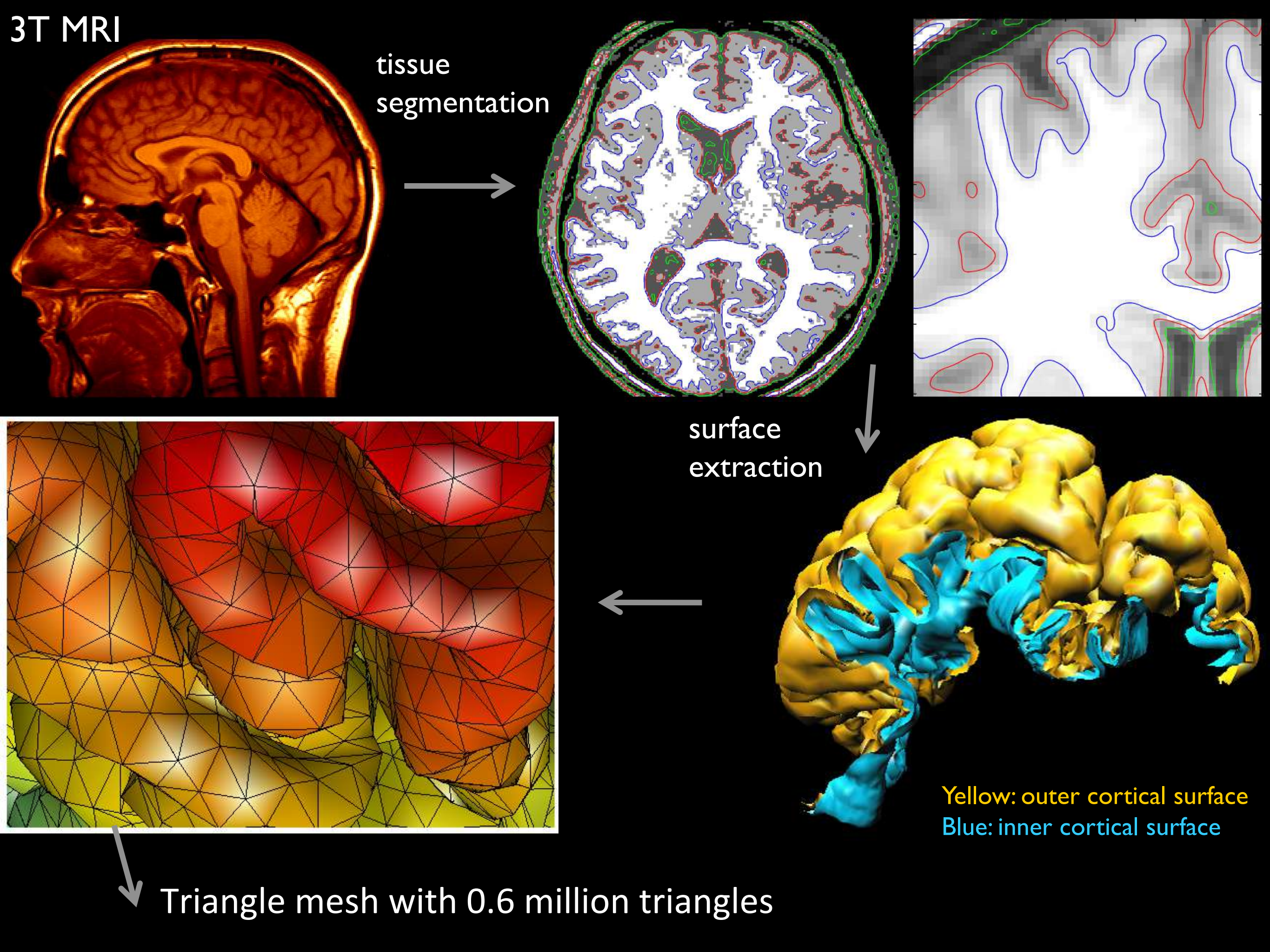
3.0 Tesla GE Scanner

Soft tissues



3D image



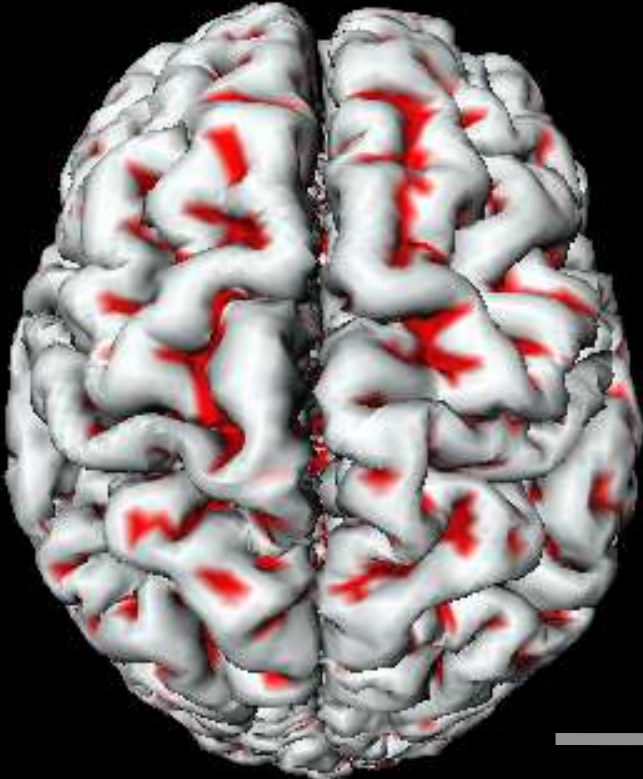


Surface parameterization

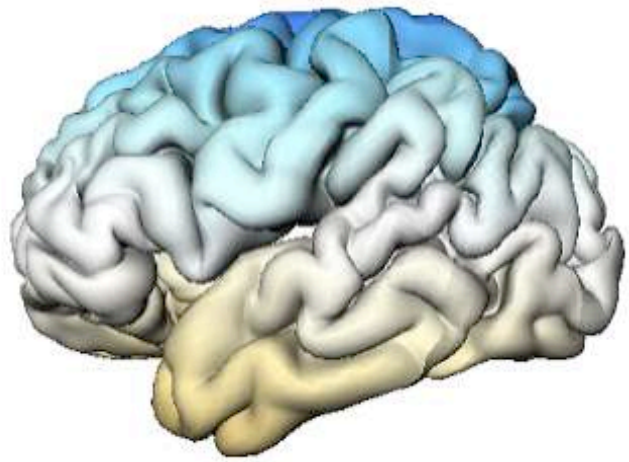
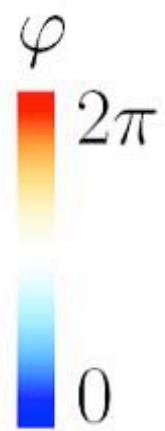
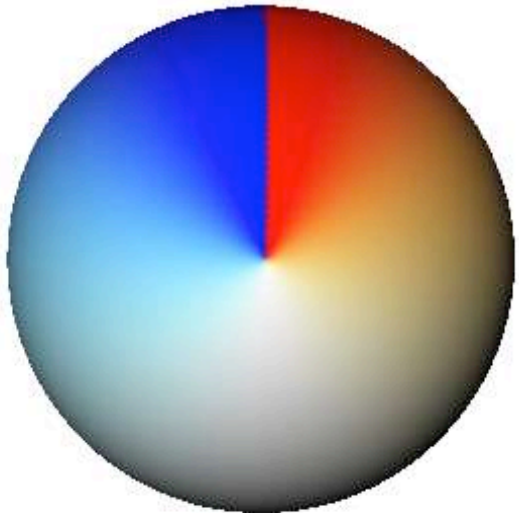
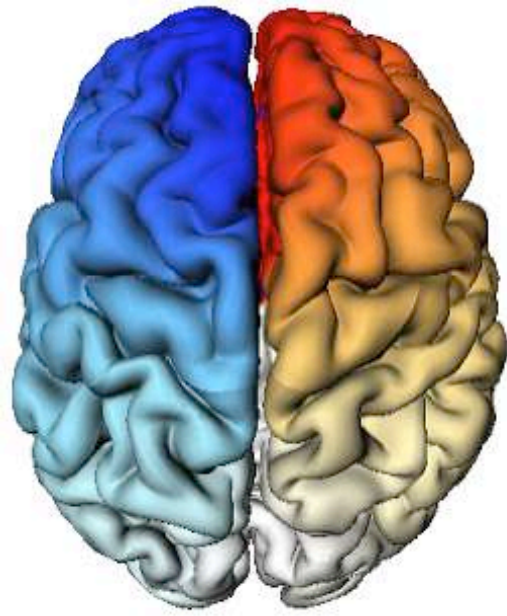
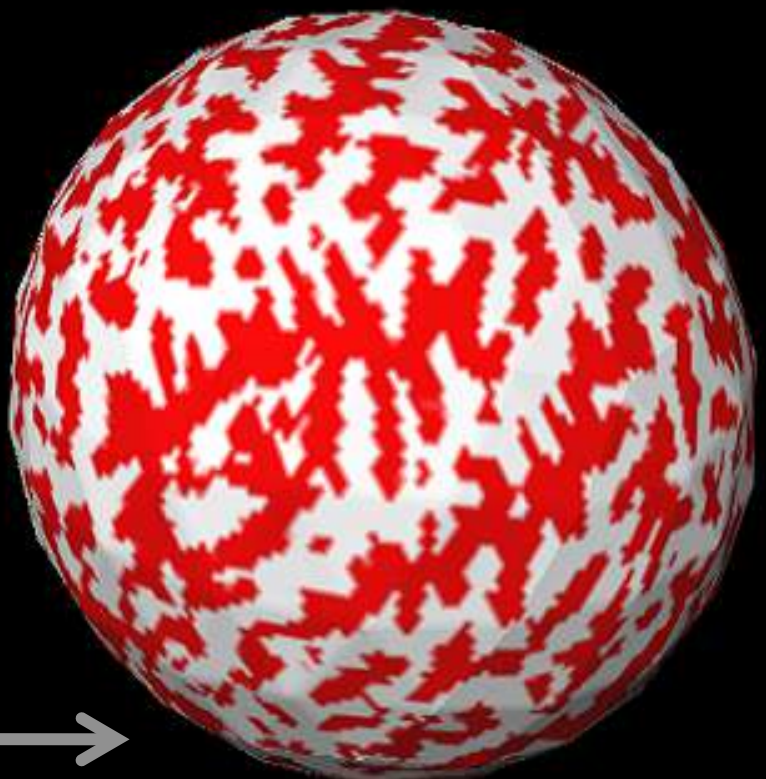
3T MRI



Surface segmentation



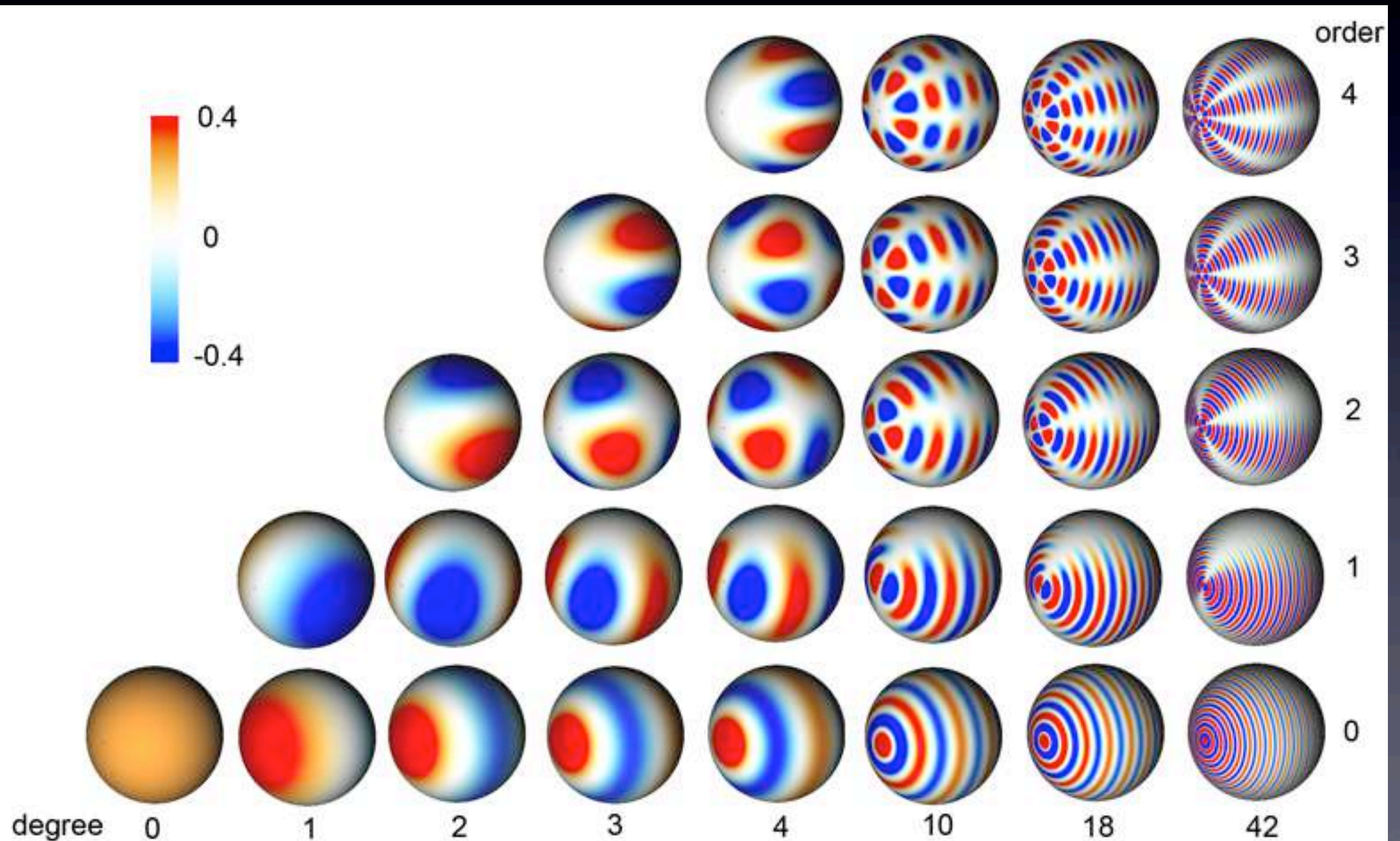
Surface flattening



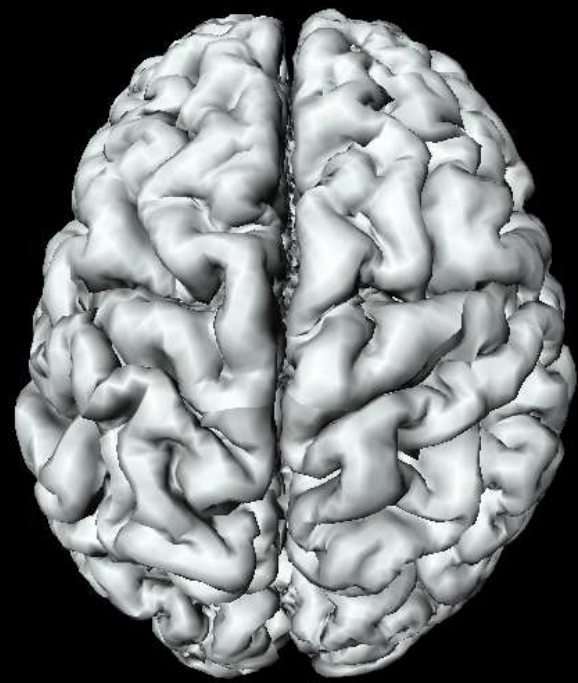
Spherical angle based coordinate system

Spherical harmonic of degree l and order m

$$Y_{lm} = \begin{cases} c_{lm} P_l^{|m|}(\cos \theta) \sin(|m|\varphi), & -l \leq m \leq -1, \\ \frac{c_{lm}}{\sqrt{2}} P_l^0(\cos \theta), & m = 0, \\ c_{lm} P_l^{|m|}(\cos \theta) \cos(|m|\varphi), & 1 \leq m \leq l, \end{cases}$$



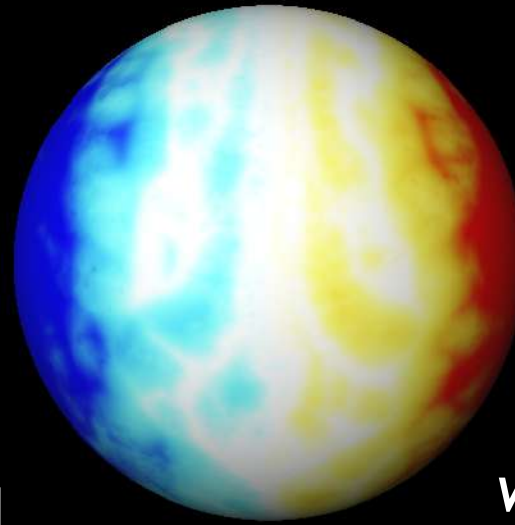
Weighted-Spherical harmonics (SPHARM)



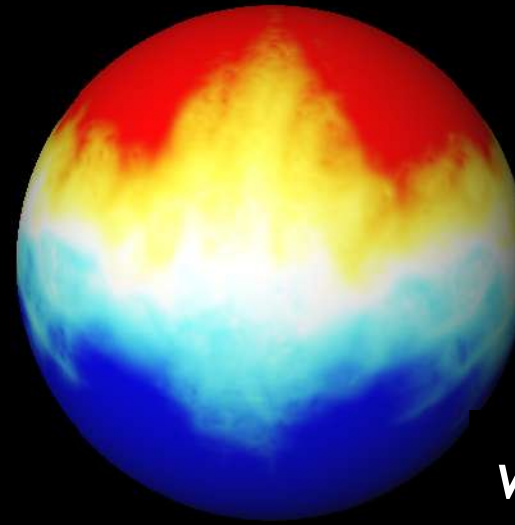
Surface
flattening



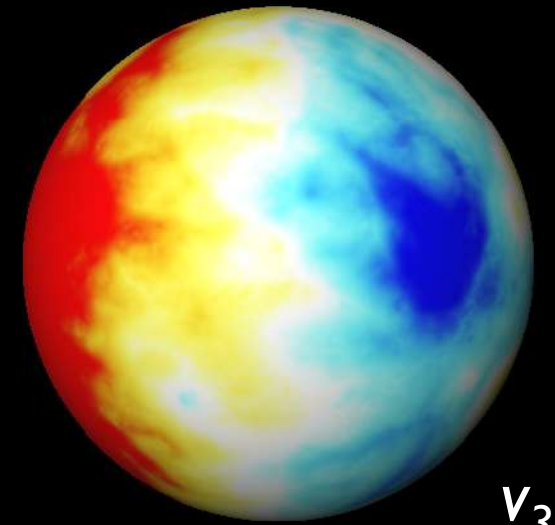
Coordinate functions



v_1

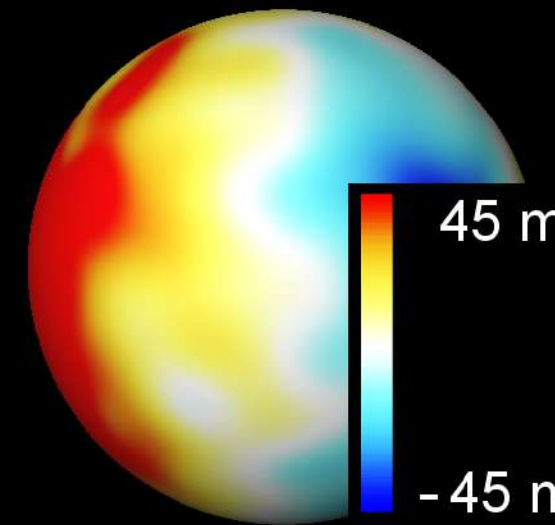
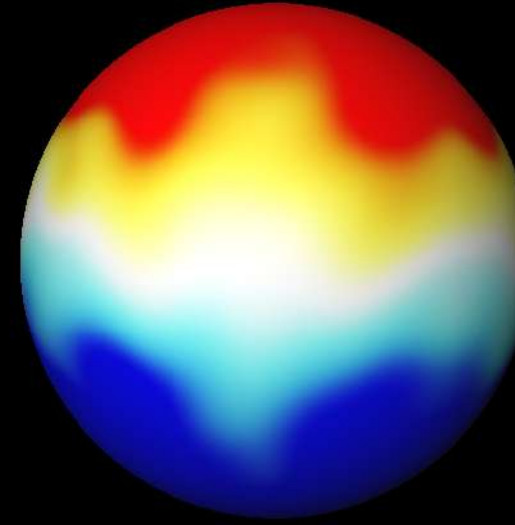
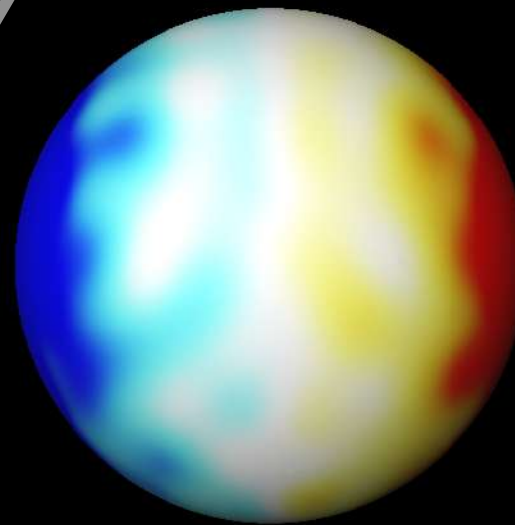


v_2



v_3

Weighted-SPHARM



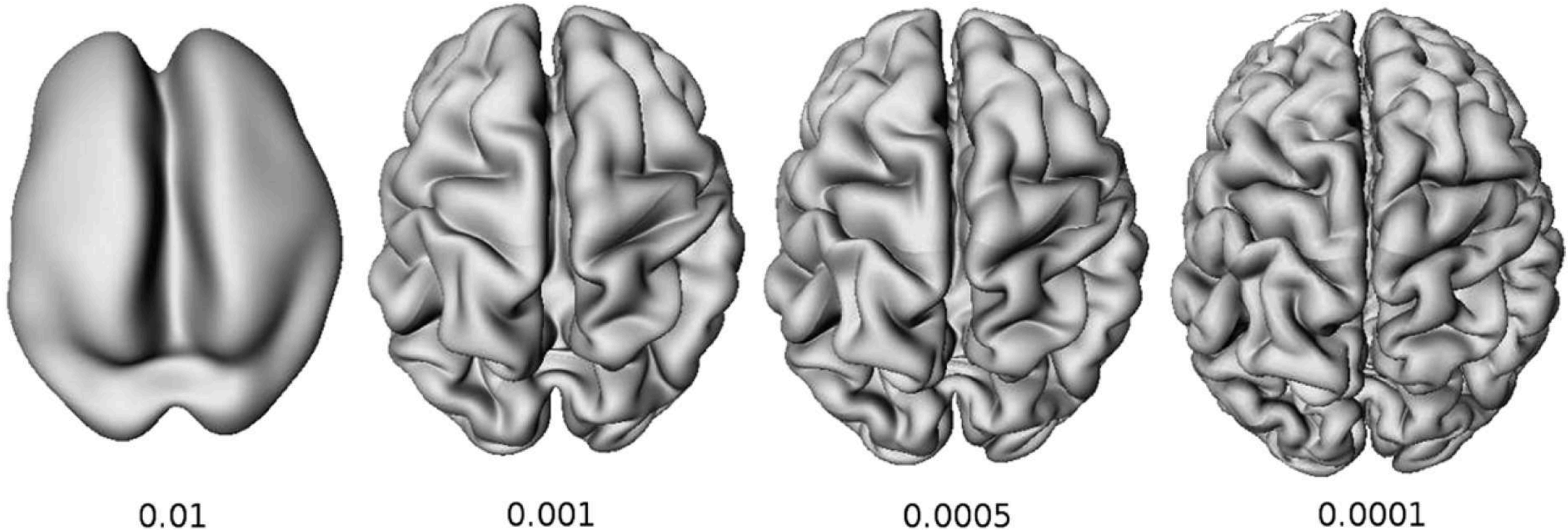
45 mm

-45 mm

$$K_{\sigma}(\theta, \phi, \theta', \phi') = \sum_{l=0}^{\infty} \sum_{m=-l}^l e^{-l(l+1)\sigma} Y_{lm}(\theta, \phi) Y_{lm}(\theta', \phi')$$

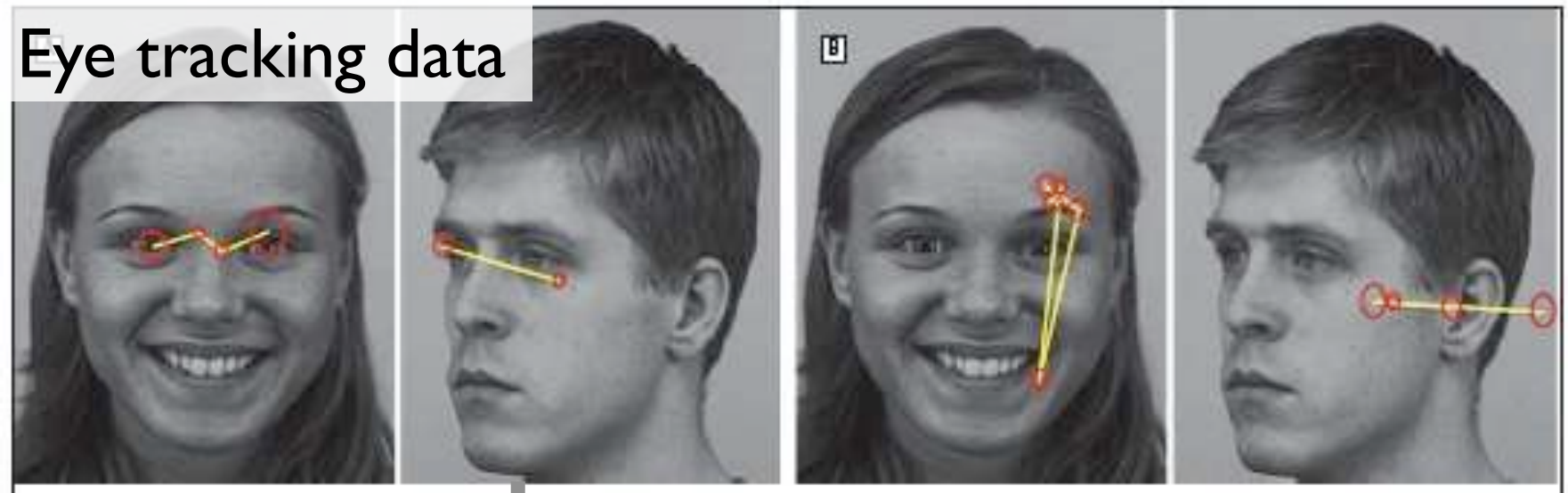
$$K_{\sigma} * v_i(\theta, \phi) = \int_0^{2\pi} \int_0^{\pi} K_{\sigma}(\theta, \phi, \theta', \phi') v_i(\theta', \phi') \sin \theta' d\theta' d\phi'$$

Heat kernel smoothing of surface coordinates

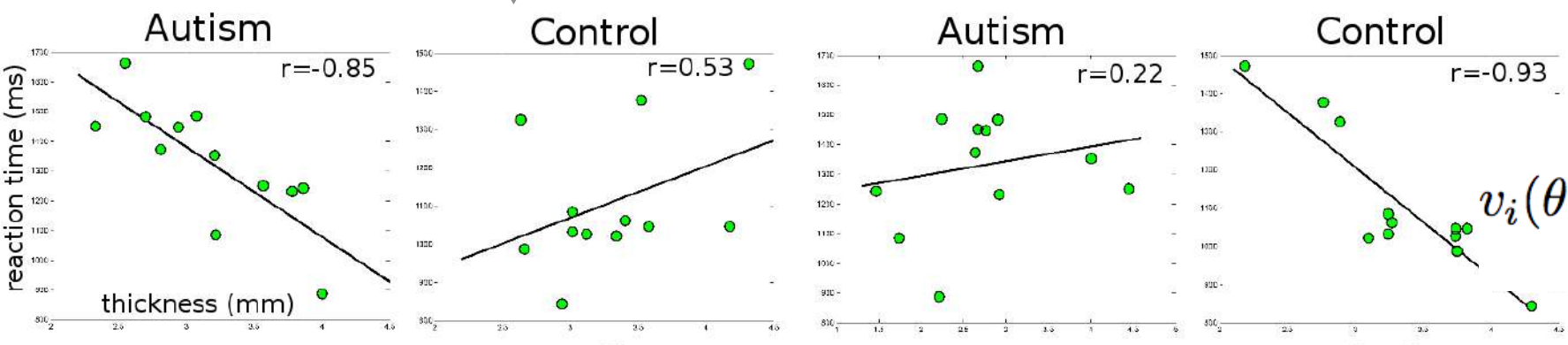


Correlating function to structure

Eye tracking data

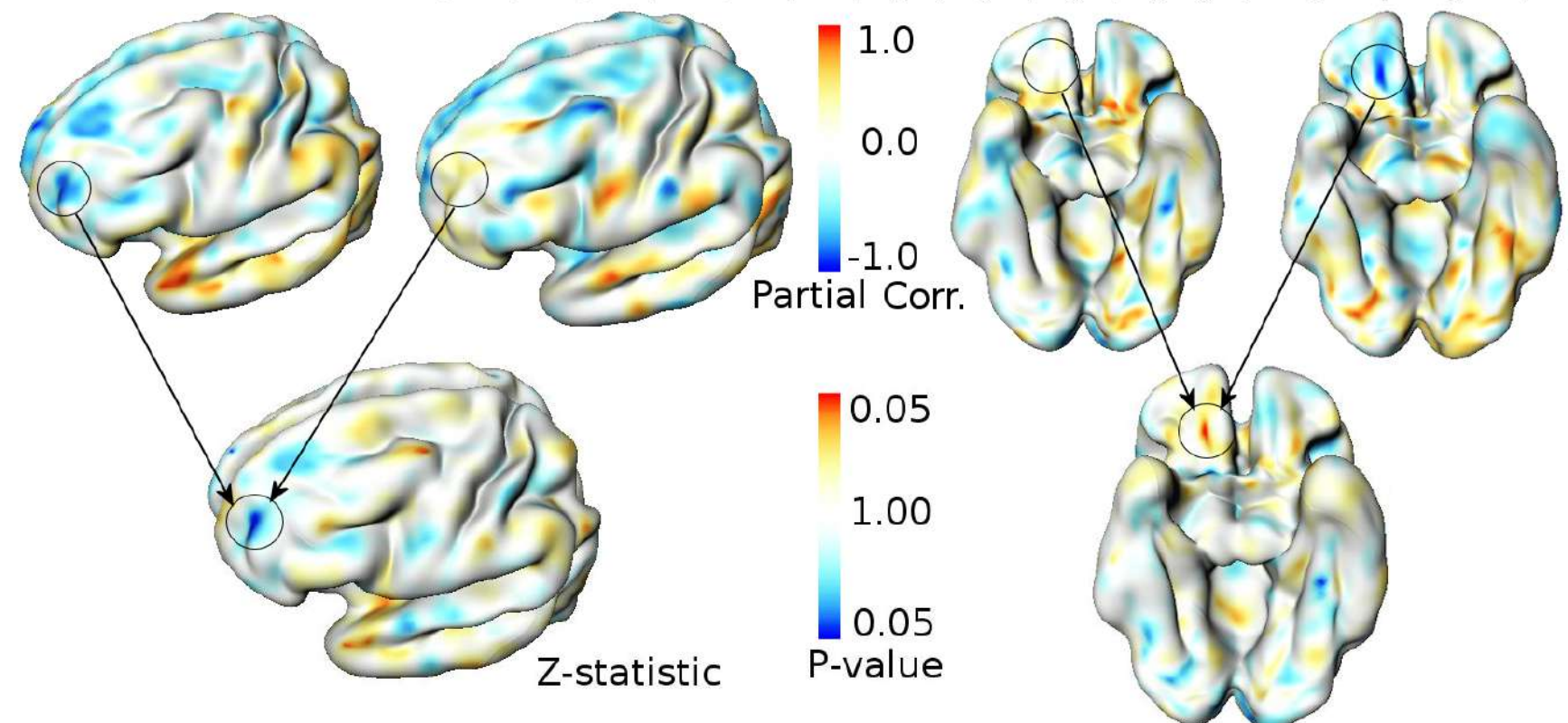


Partial correlation mapping



Weighted Fourier representation

$$v_i(\theta, \varphi) = \sum_{l=0}^k \sum_{m=-l}^l e^{-l(l+1)\sigma} f_{lm}^i Y_{lm}(\theta, \varphi)$$



88.1799	56.6336	5.7367
-12.4775	-11.2552	-2.0791
2.4336	-15.4428	-0.4021
4.3956	2.2733	-0.9354
-0.0106	-0.0674	0.6999
2.1773	-2.4194	-0.1176
0.5808	0.8390	1.2942
0.0615	-0.1893	0.1188
-0.2629	0.7524	0.1089
0.7909	-0.7276	-0.1901
0.5458	0.6236	0.6939

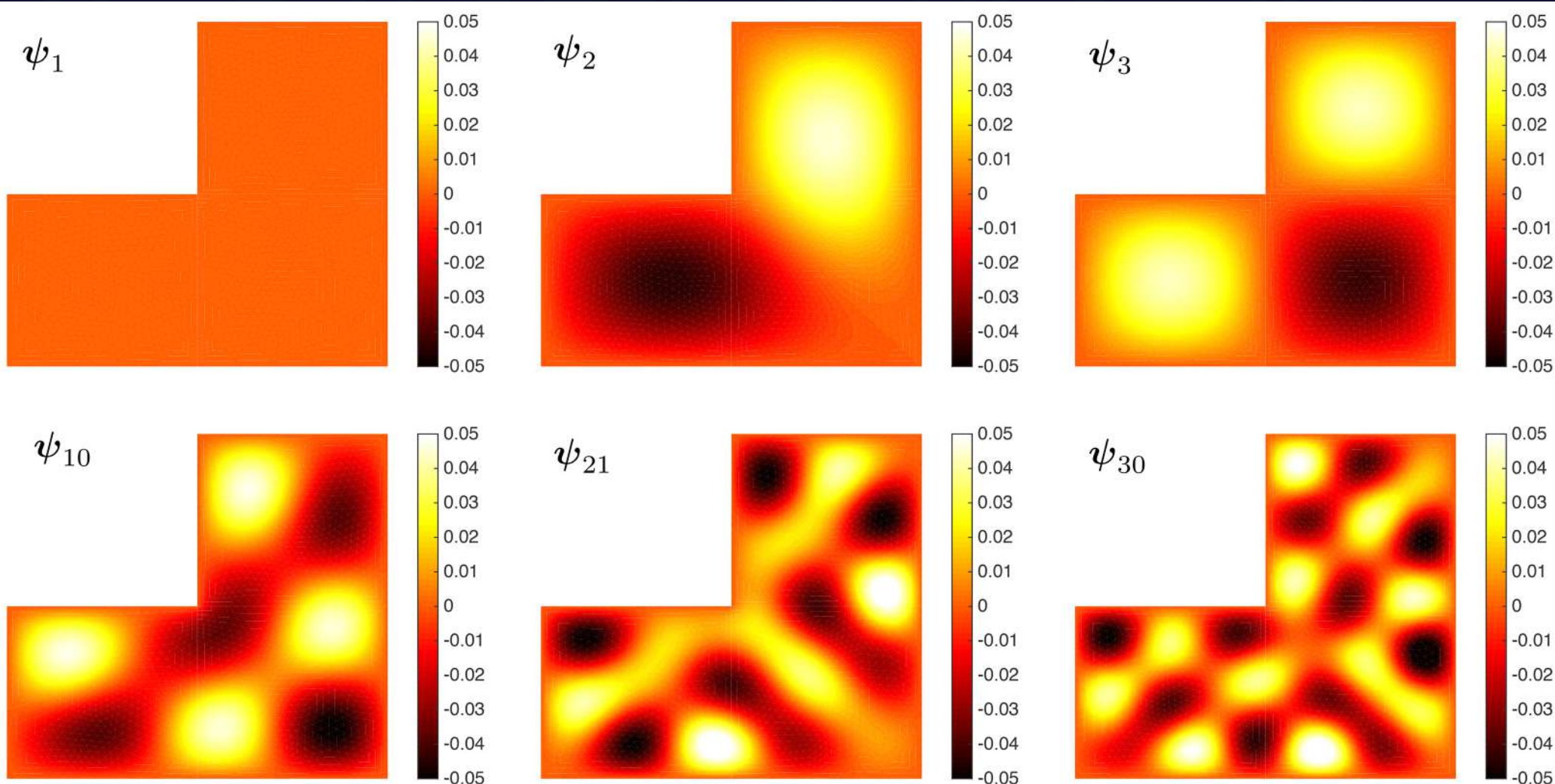
.....

Heat kernel smoothing
using LB-eigenfunctions

Basis in an arbitrary domain

Steady-state oscillations in a wave equation

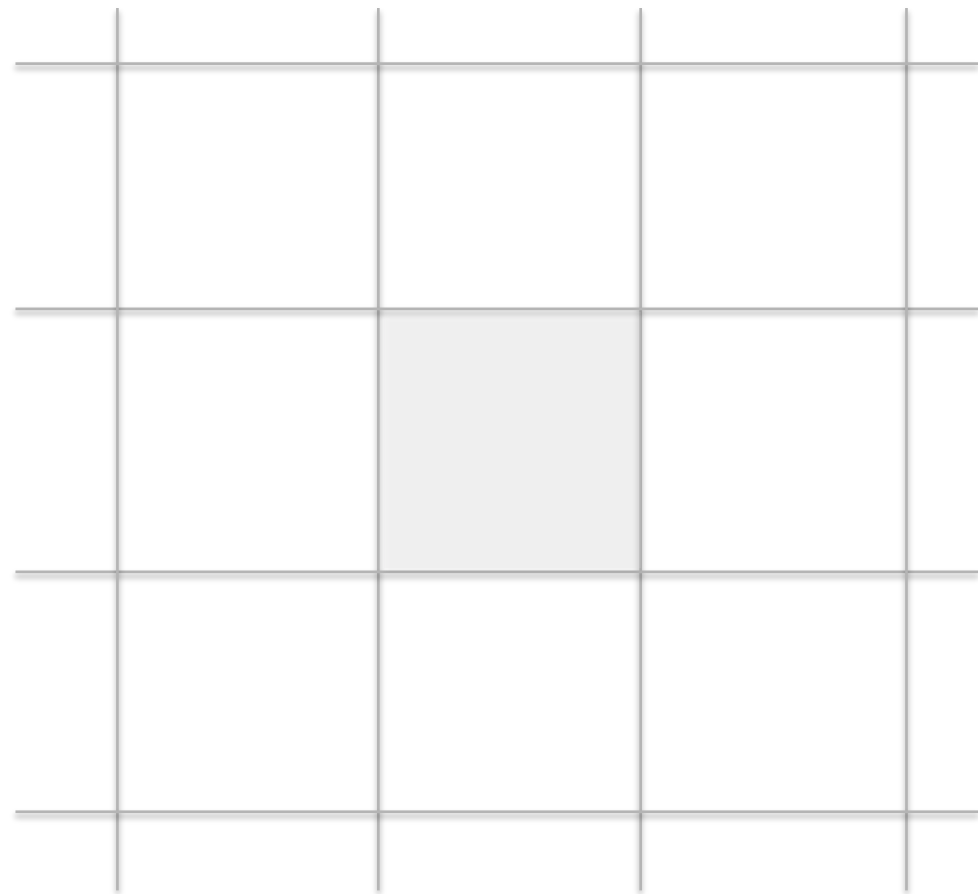
Helmholtz equation $\Delta_X F = \lambda F$



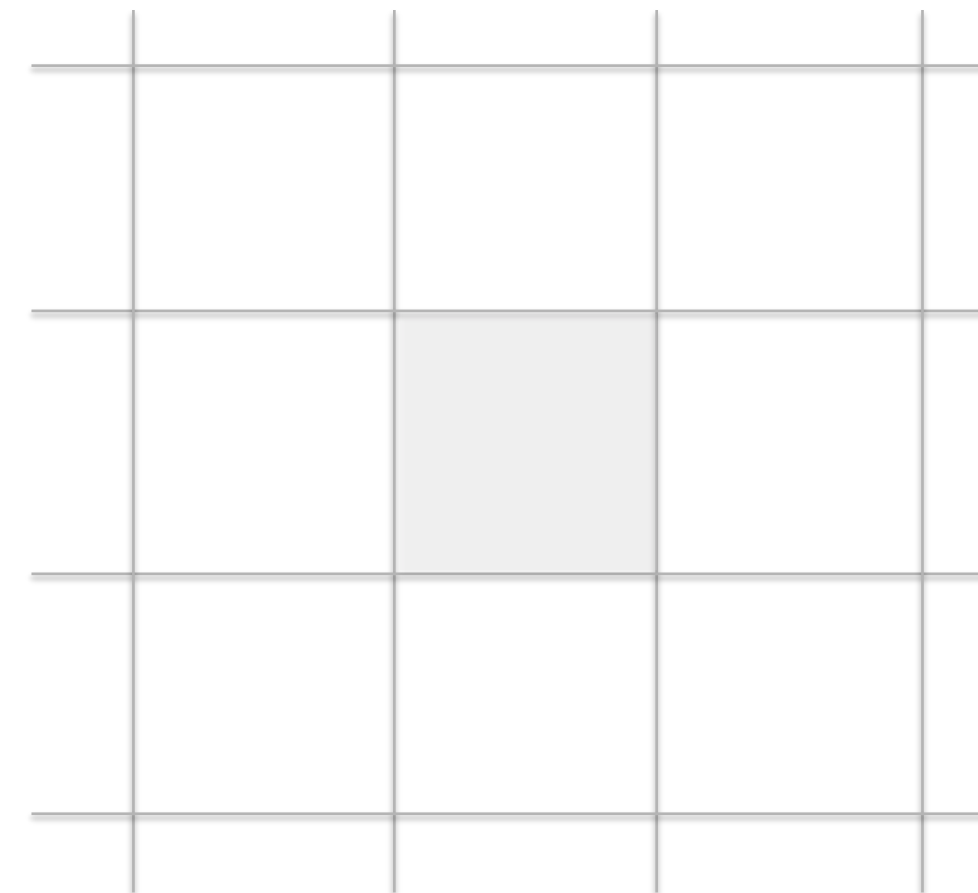
Orthonormal
Basis

6 nearest neighbors in 3D

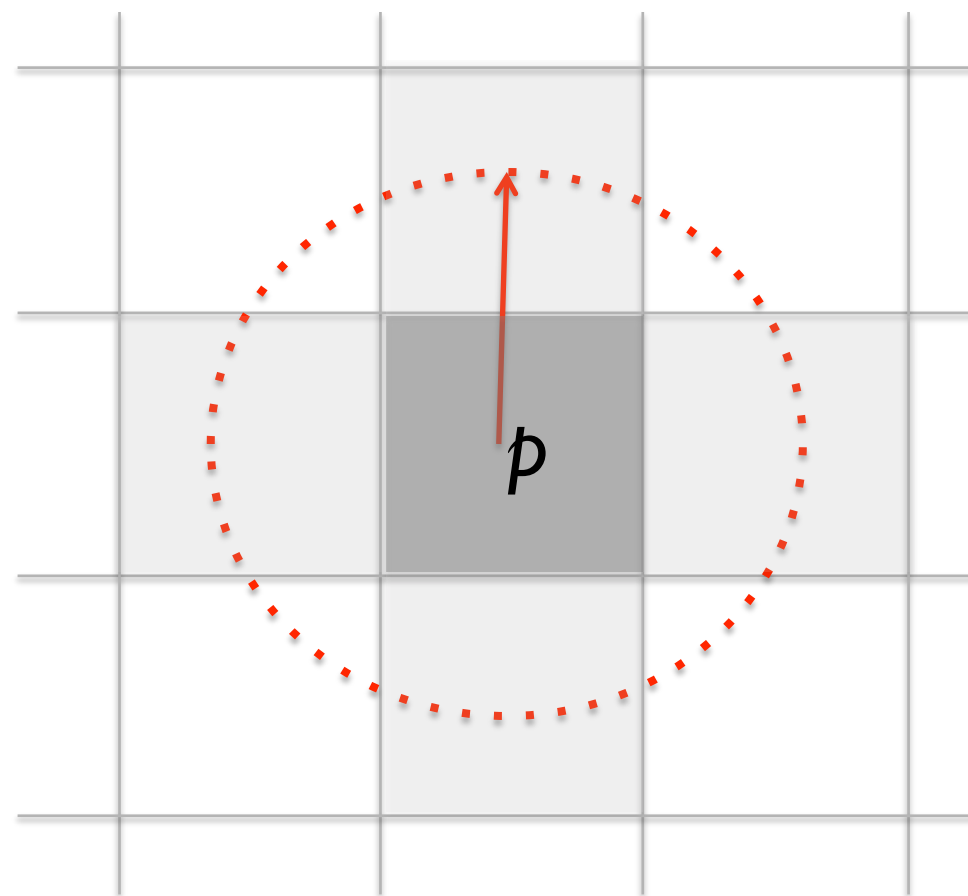
Top layer



Bottom layer



Middle layer

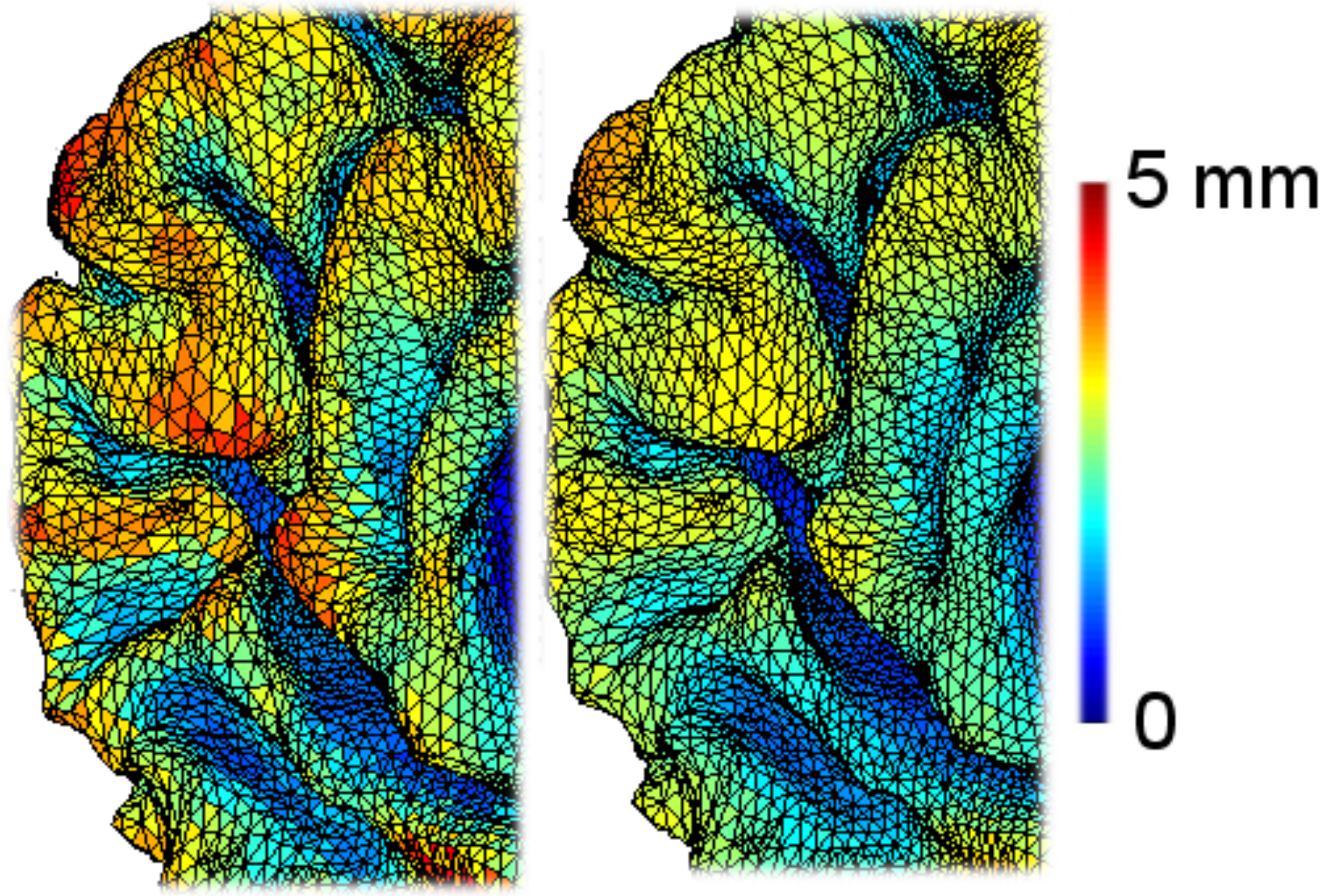


Connect any neighboring voxel with distance less than l

$$\Delta f(p) = \frac{\partial^2 f}{\partial x^2} + \frac{\partial^2 f}{\partial y^2} + \frac{\partial^2 f}{\partial z^2}$$

$$\Delta f(p) = \sum_{\delta p} f(p + \delta p) - 6f(p)$$

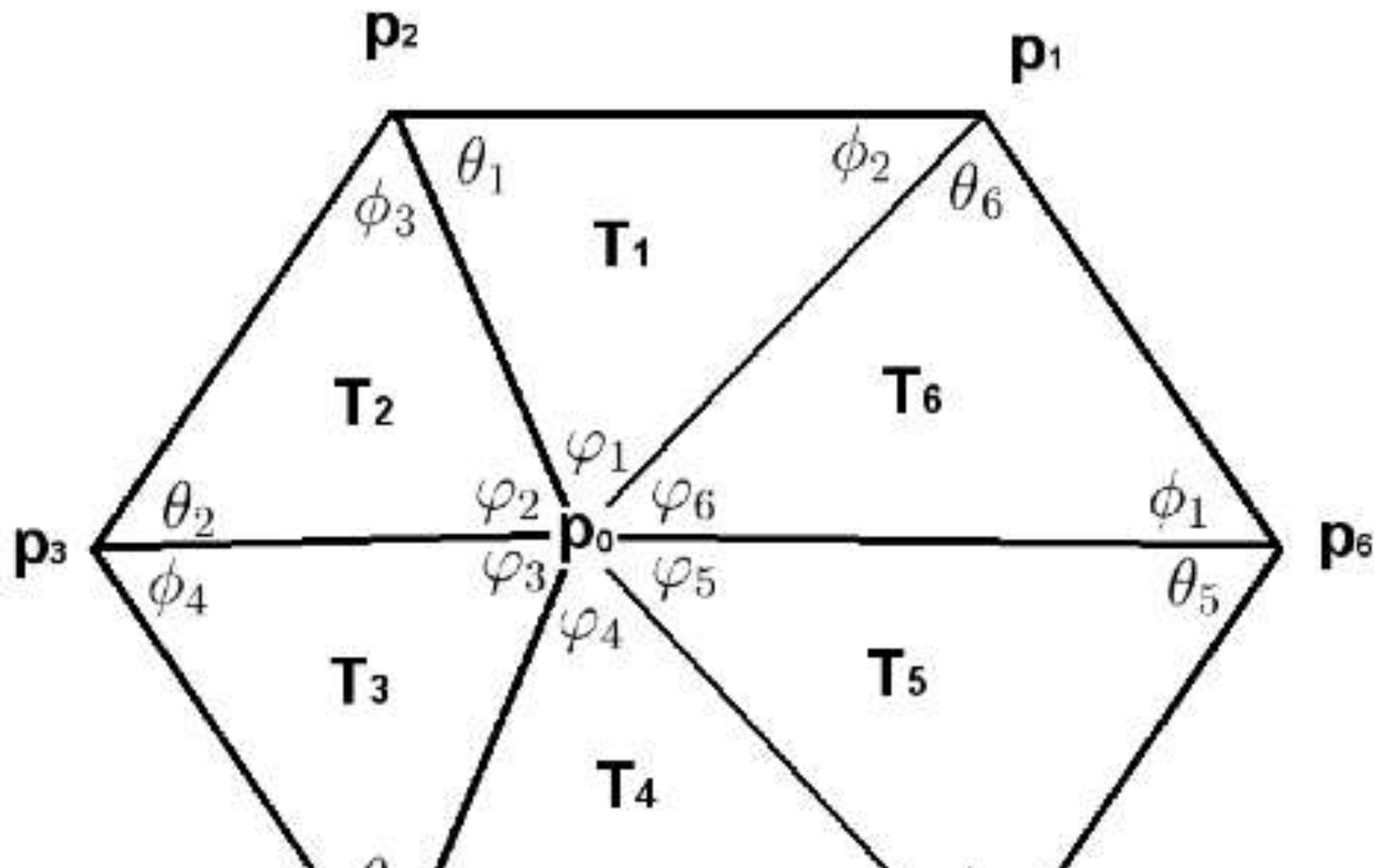
Surface data on triangle meshes



measurement

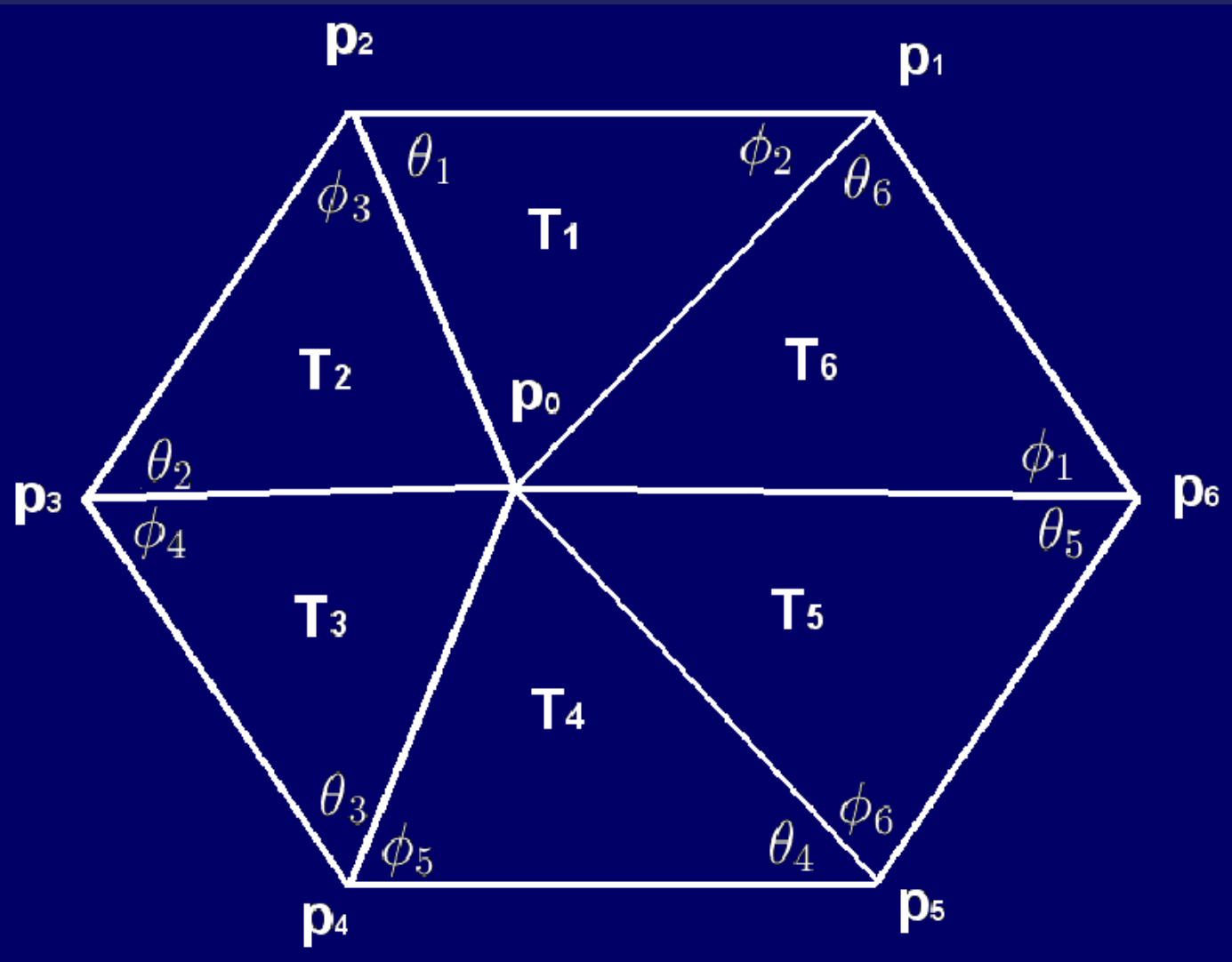
after smoothing

First order neighbor in a triangle mesh



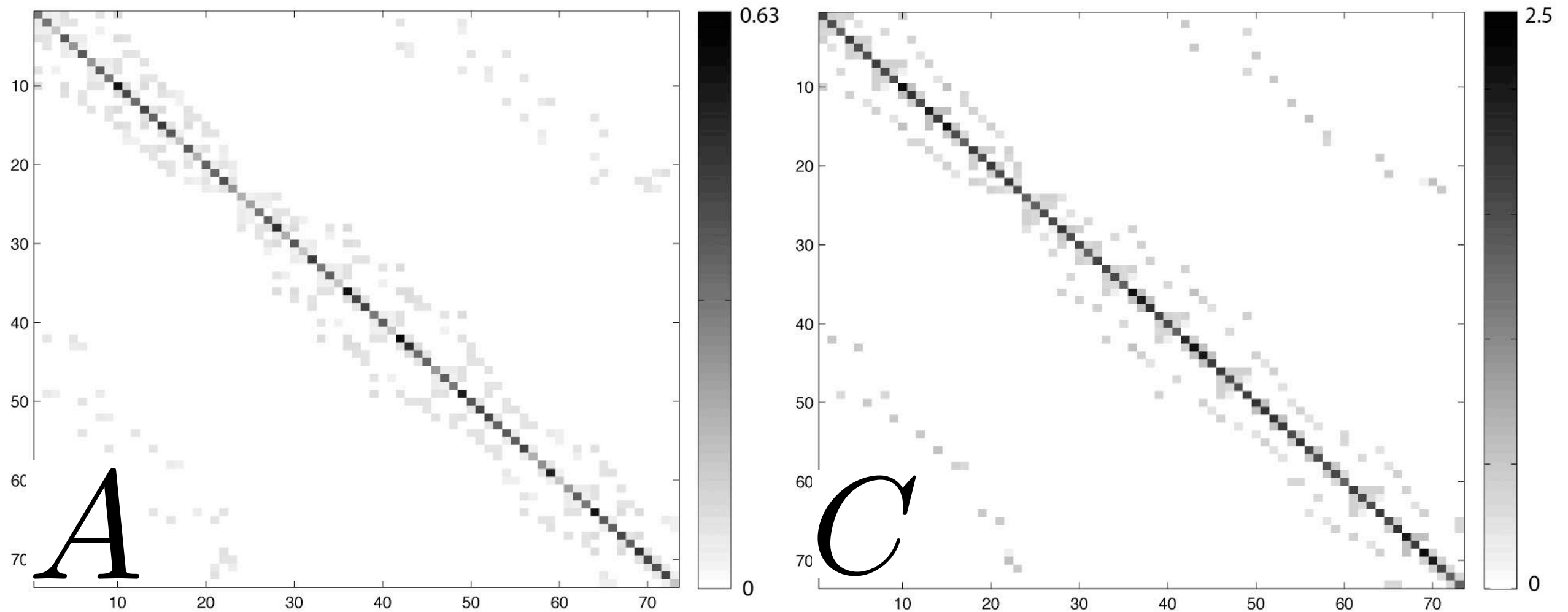
$$\Delta = \frac{1}{\det g^{1/2}} \sum_{i,j=1}^2 \frac{\partial}{\partial u^i} \left(\det g^{1/2} g^{ij} \frac{\partial}{\partial u^j} \right)$$

Cotan Discretization



$$\Delta f(p) = \sum_{i=1}^m w_i [f(p_i) - f(p)]$$

$$w_j = \frac{\cot \theta_j + \cot \phi_j}{\sum_{j=1}^m |T_j|}$$



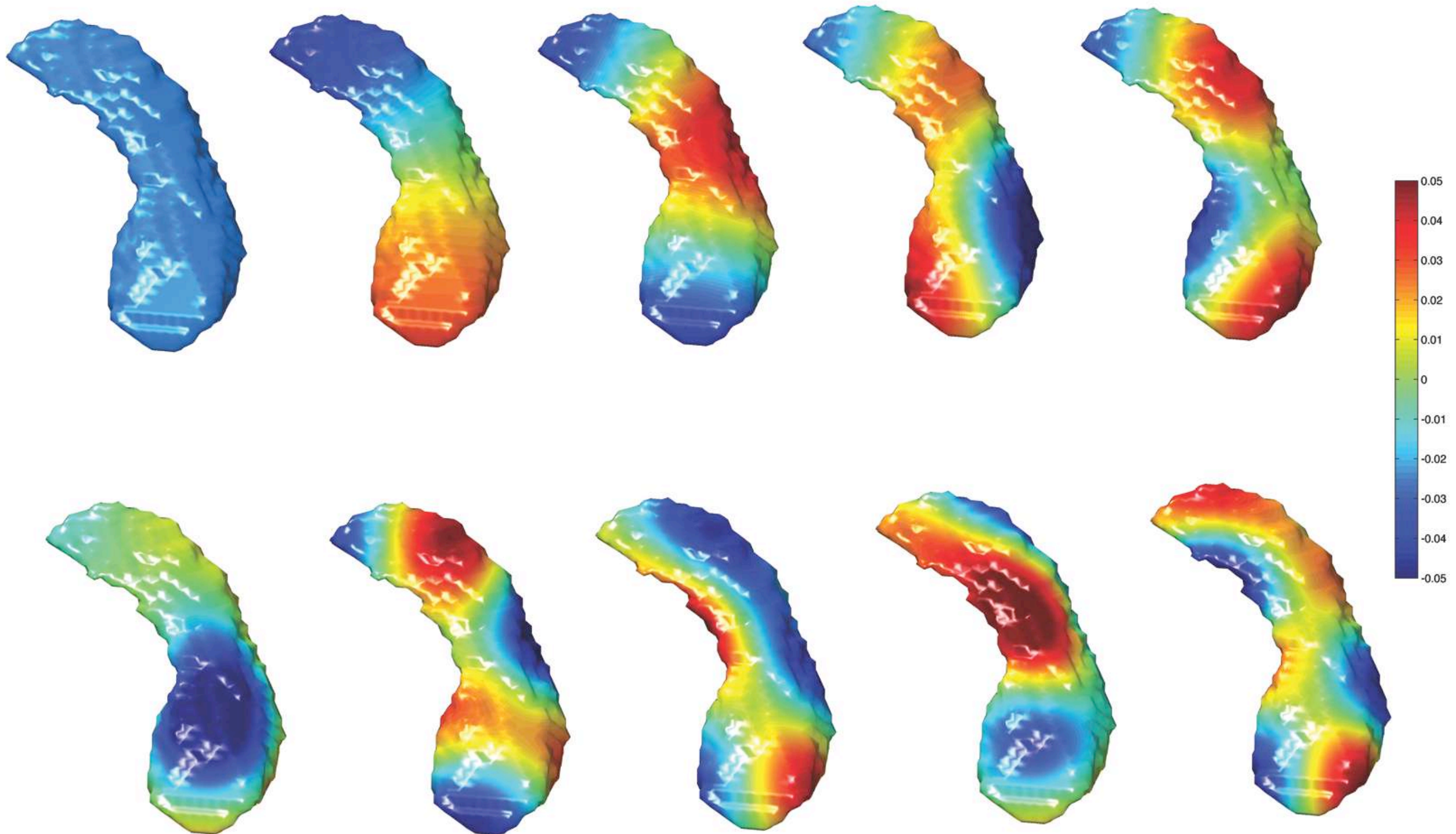
$$\Delta f = \lambda f \longrightarrow C\psi = \lambda A\psi$$

MATLAB code:

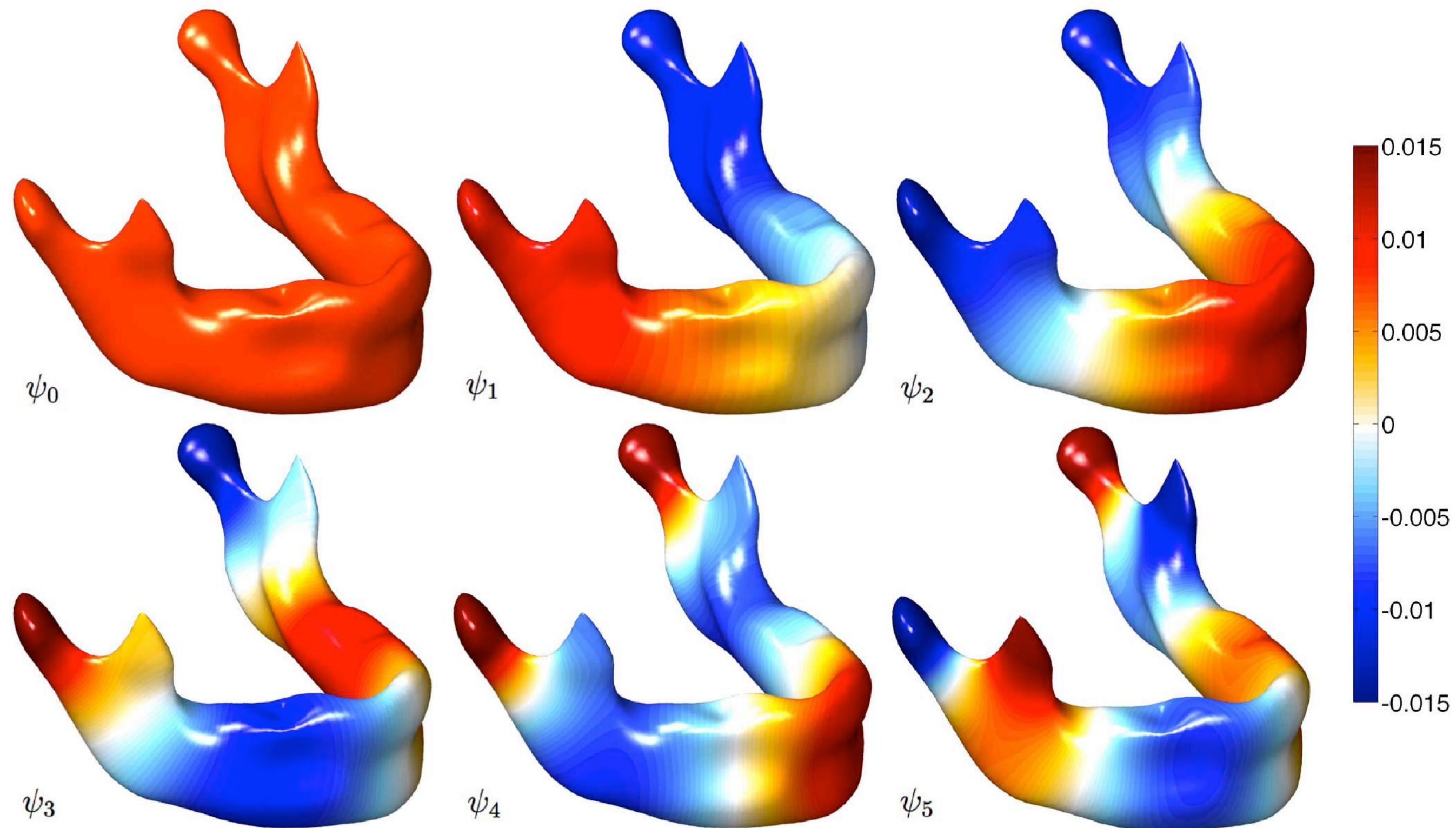
<http://brainimaging.waisman.wisc.edu/~chung/lb>

Tested for meshes with up to half million vertices

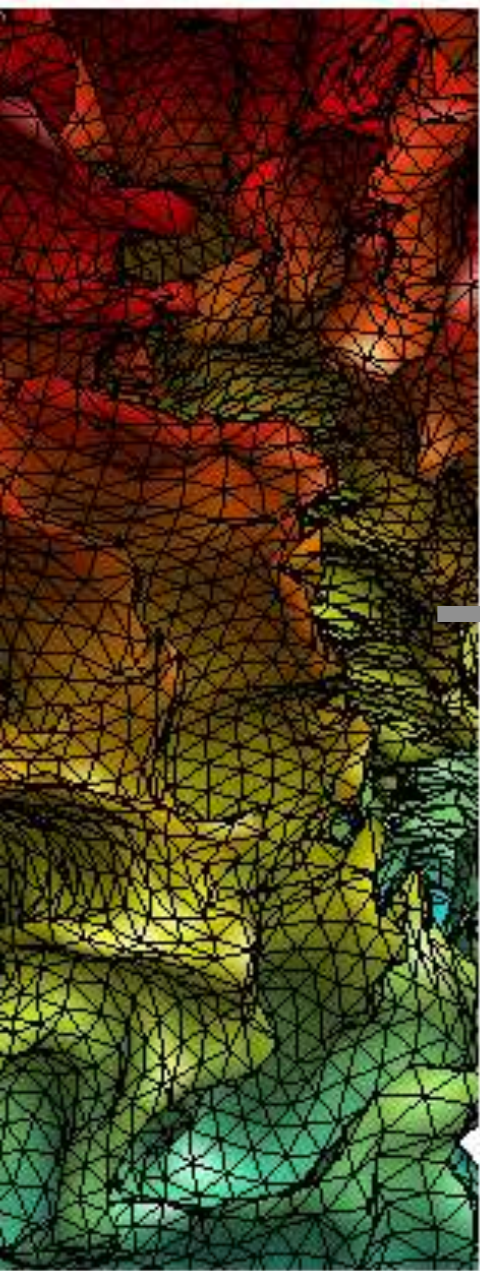
First 10 LB-eigenfunctions on left hippocampus



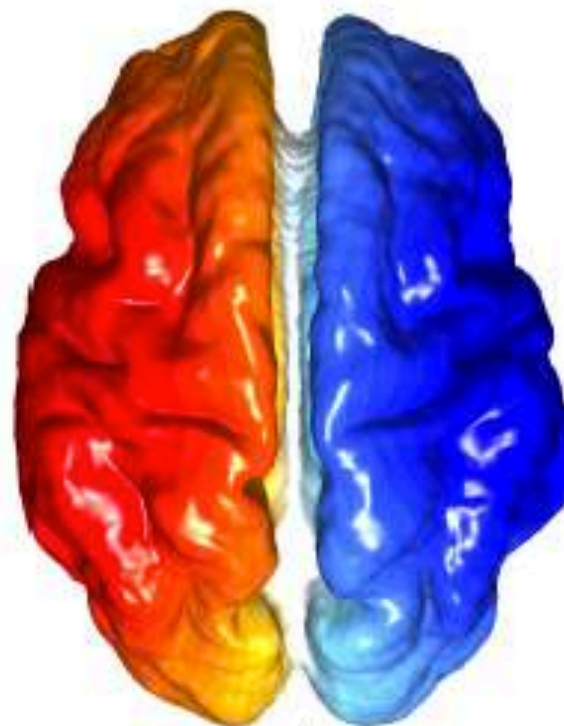
LB-eigenfunctions on mandible $\Delta f = \lambda f$



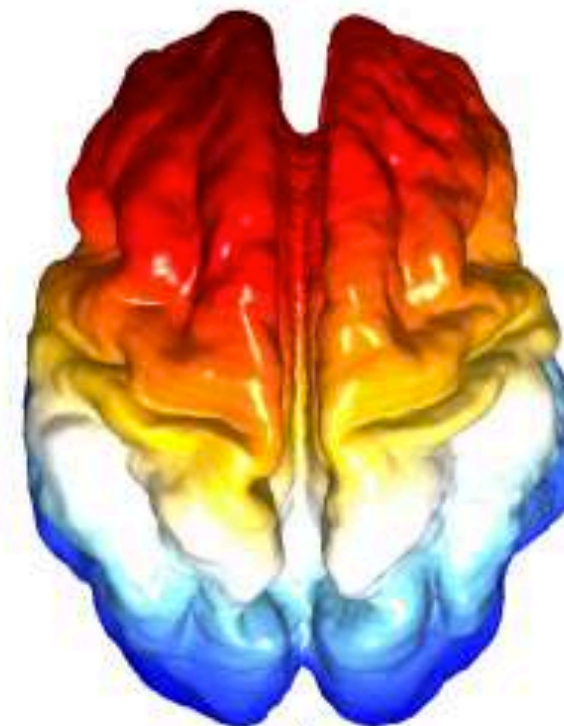
LB-eigenfunctions on brain surface $\Delta f = \lambda f$



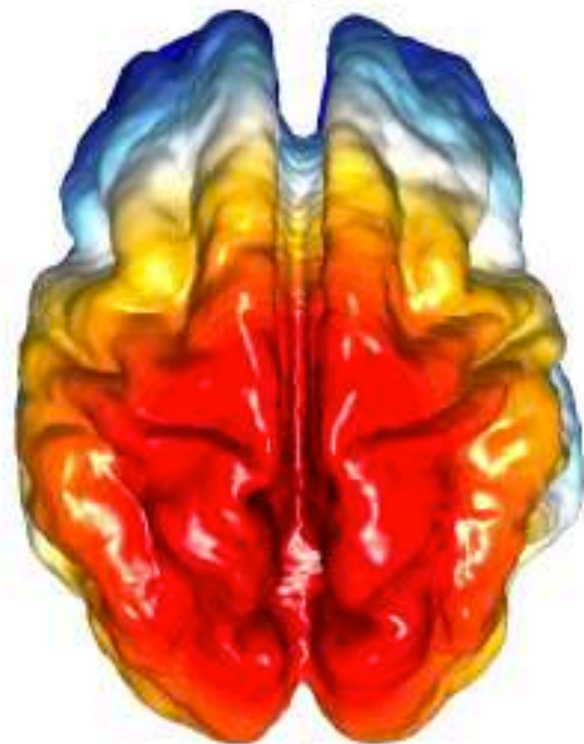
ψ_0



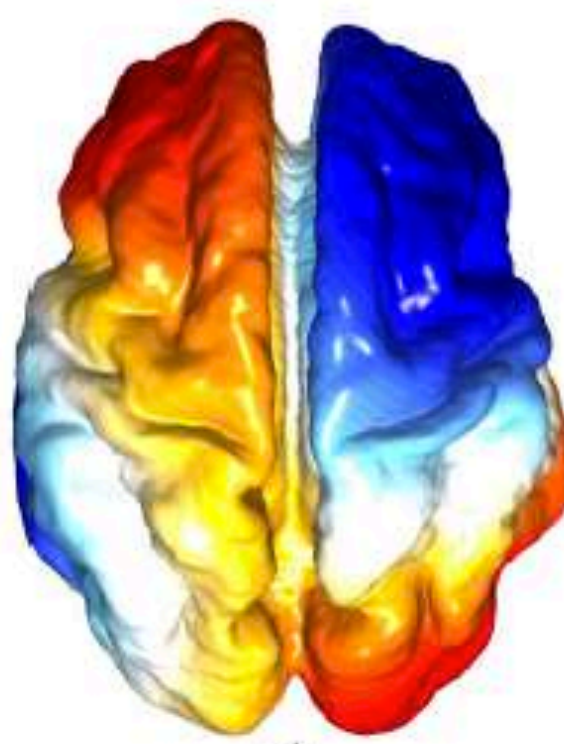
ψ_1



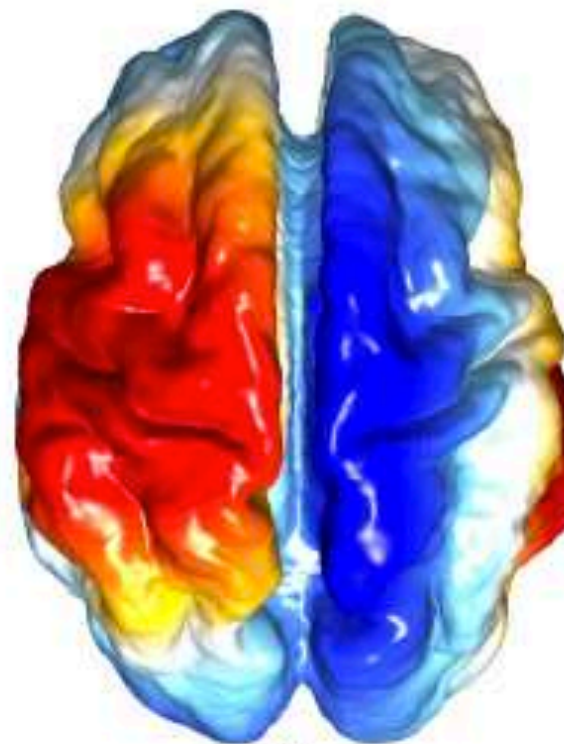
ψ_2



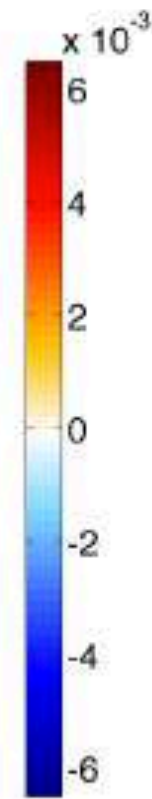
ψ_3



ψ_4

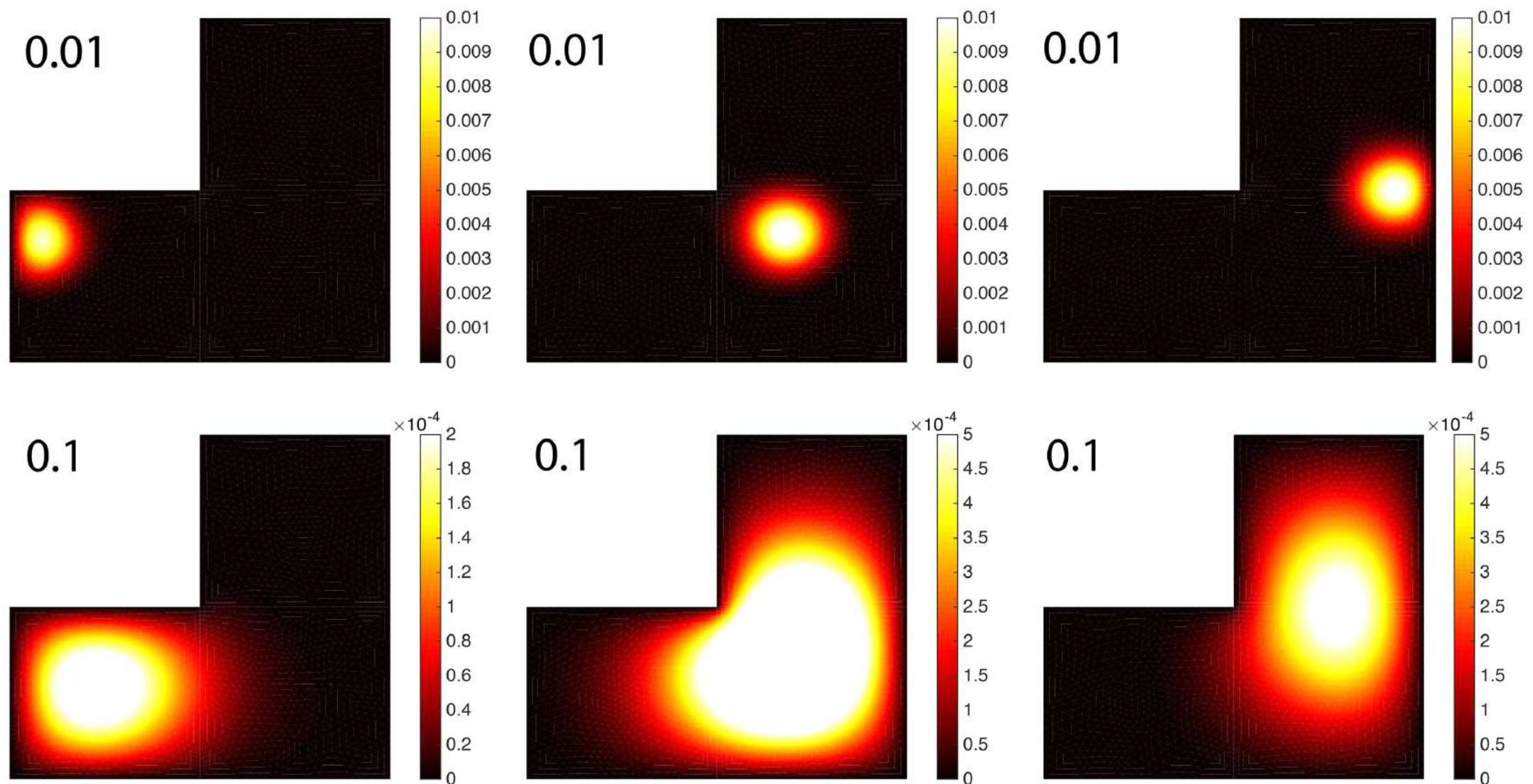


ψ_5



Heat kernel

$$K_\sigma(p, q) = \sum_{j=0}^{\infty} e^{-\lambda_j \sigma} \psi_j(p) \psi_j(q)$$



Fundamental solution of isotropic diffusion on manifolds

Diffusion via heat kernel smoothing

Diffusion equation $\frac{\partial f}{\partial t} = \Delta f, f(x, t = 0) = X(x)$

$$\sigma = \sqrt{2t}$$

Heat kernel smoothing $f = K_\sigma * X$

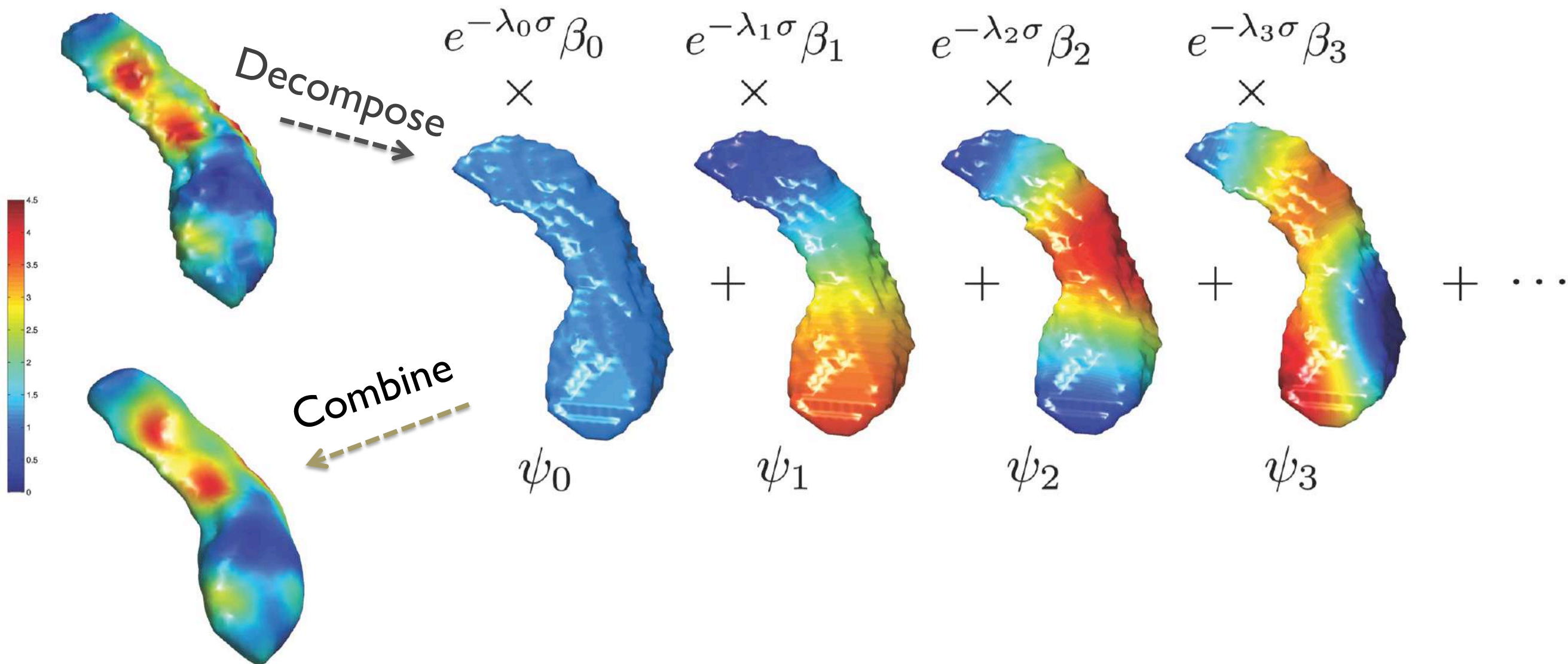
$$K_\sigma(p, q) = \sum_{j=0}^{\infty} e^{-\lambda_j \sigma} \psi_j(p) \psi_j(q)$$

Heat kernel smoothing on manifolds

$$\begin{aligned} K_\sigma * X(p) &= \int_{\mathcal{M}} K_\sigma(p, q) f(q) d\mu(q) \\ &= \sum_{j=0}^{\infty} e^{-\lambda_j \sigma} \beta_j \psi_j(p) \end{aligned}$$

Fourier coefficients

$$\beta_j = \int_{\mathcal{M}} X(p) \psi_j(p) d\mu(p)$$



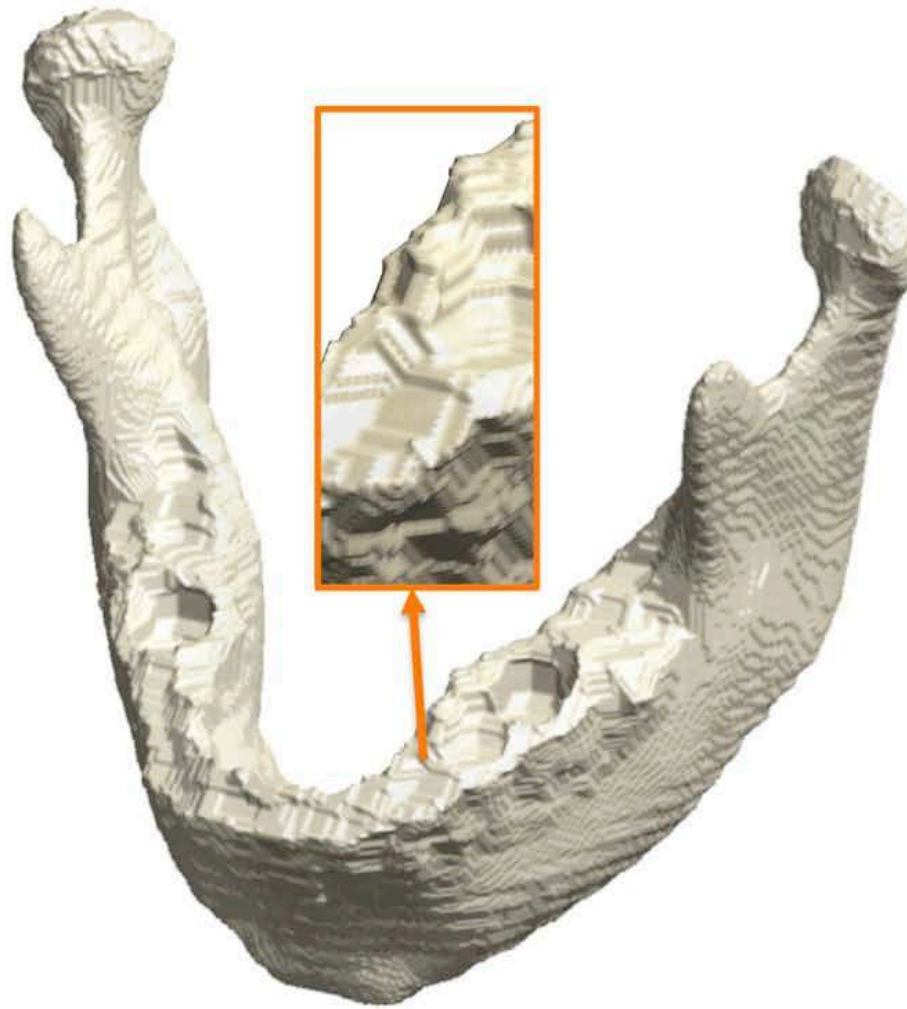
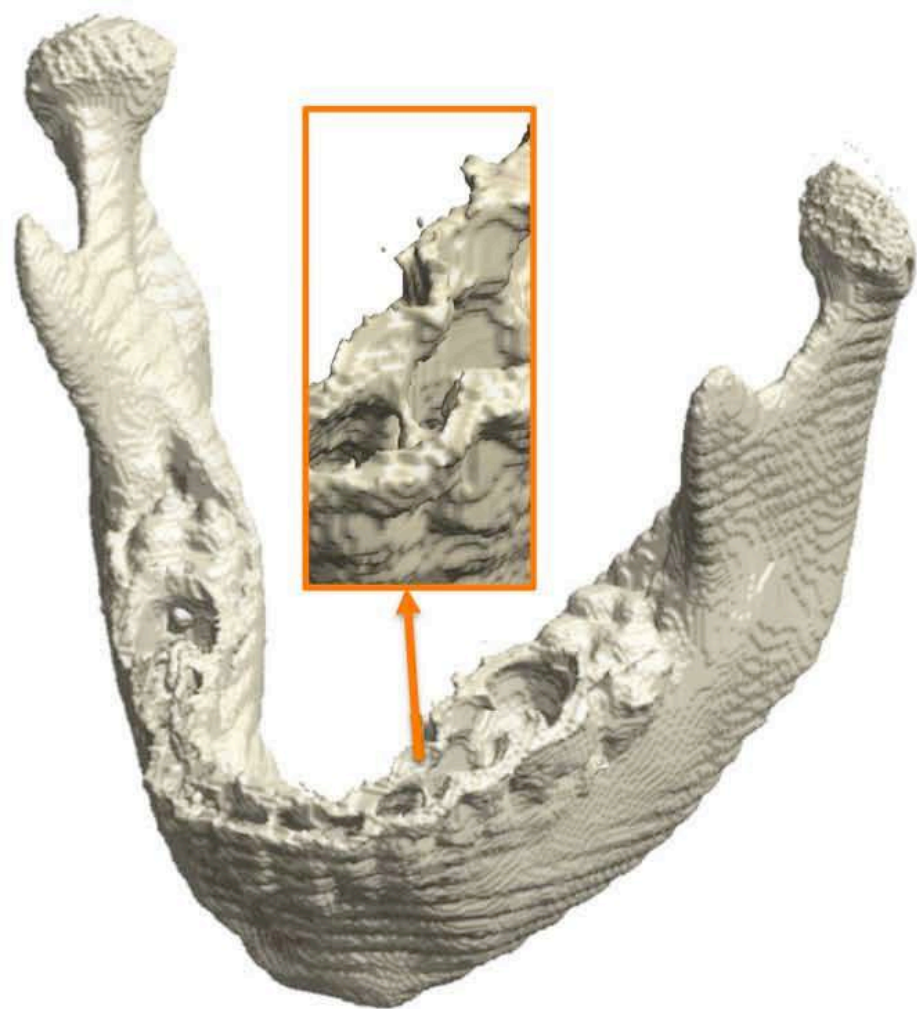
Mandible Growth Modeling from CT

Computed Tomography (CT)



Hard tissues: bones, teeth

Topology correction in CT



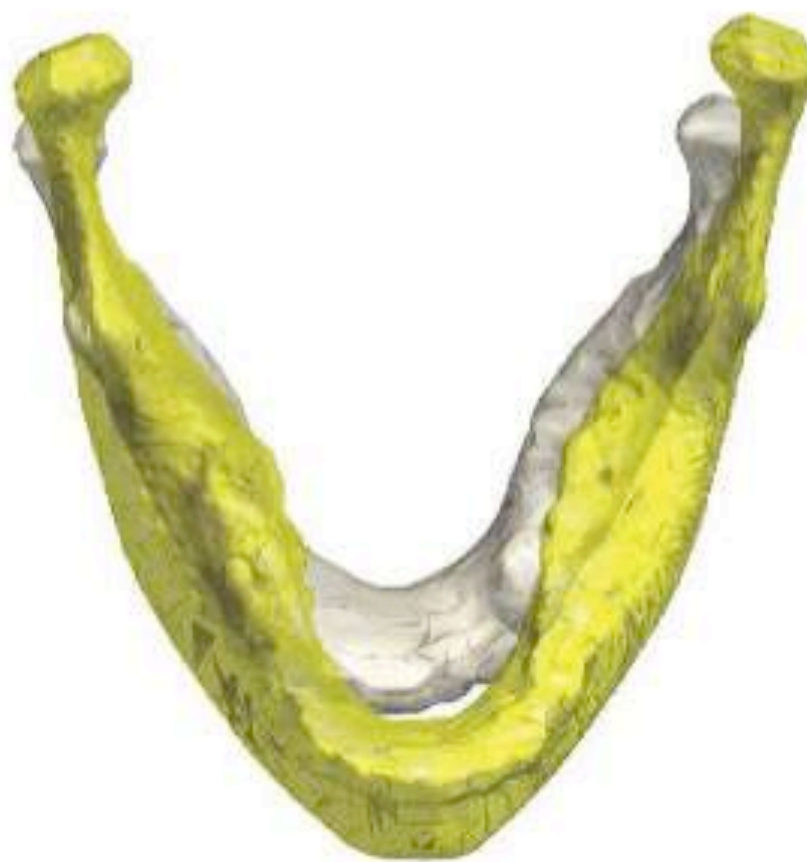
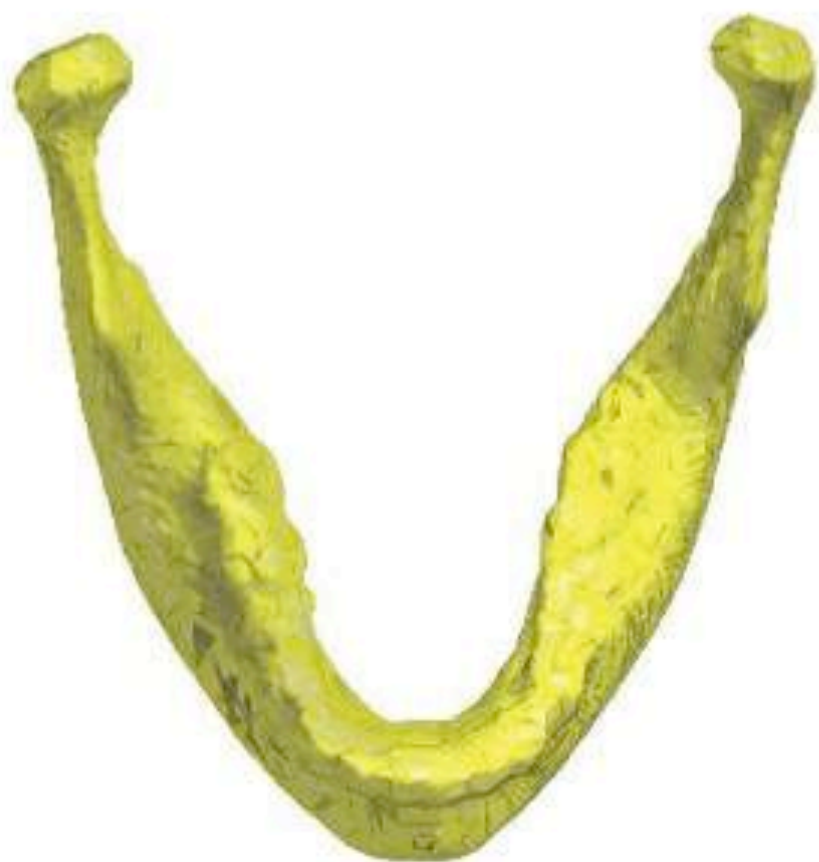
Hole & handles
corrected using
Euler characteristic

Initial affine registration

F155-12-08

F203-01-03

Affine transform
of F203-01-03



Nonlinear diffeomorphic registration

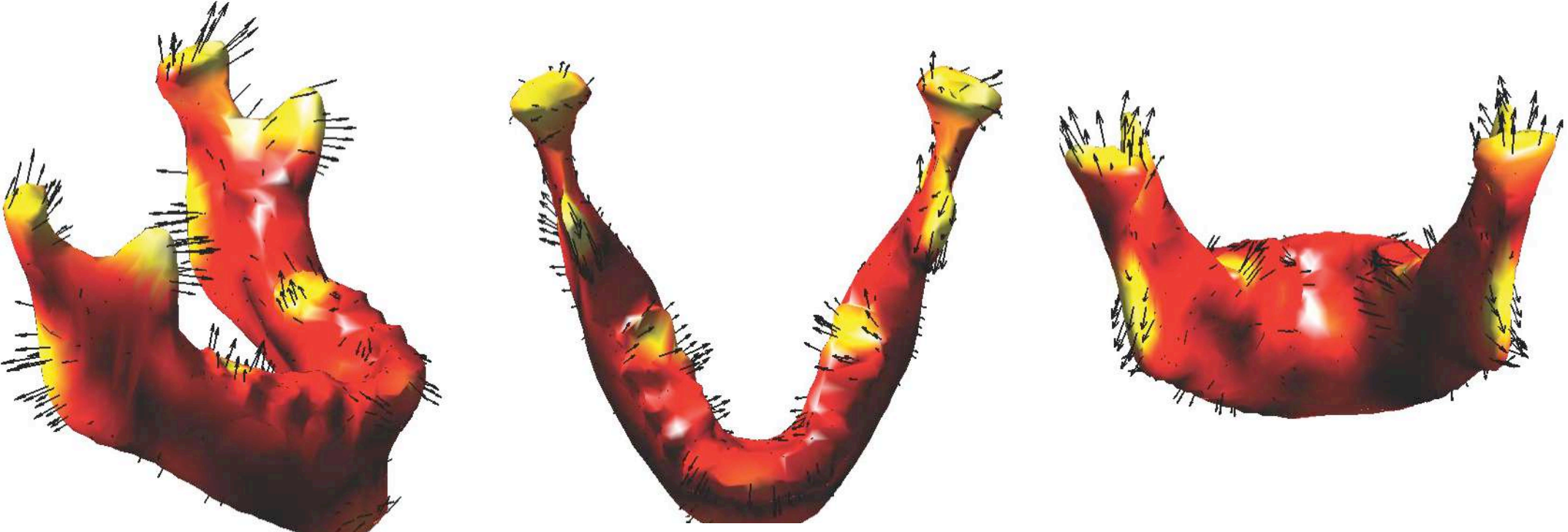


F155-12-08

Affine registered
surfaces

Final diffeomorphic
registration

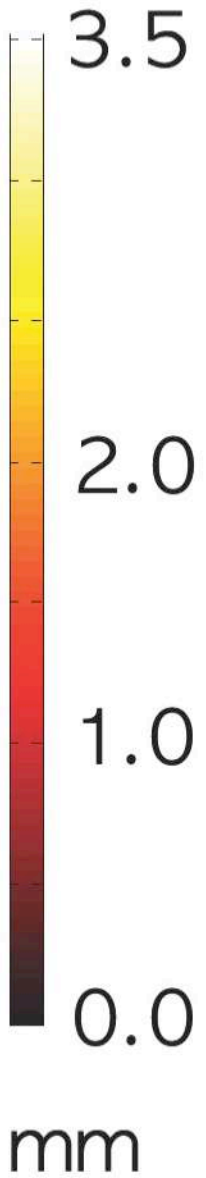
Average mandible growth pattern in children



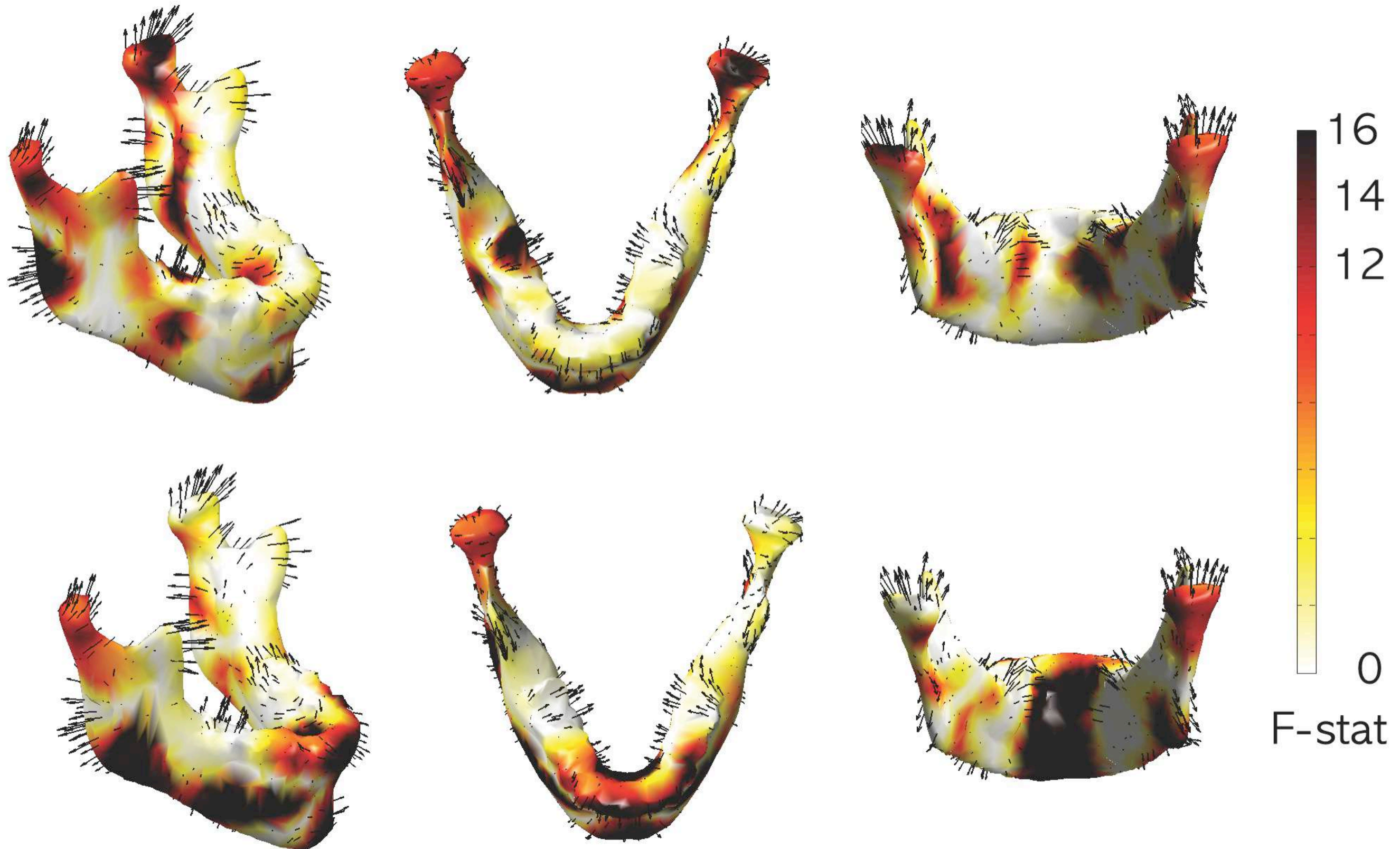
Between ages 0-6 and ages 7-12



Between age 7-12 and age 13-19



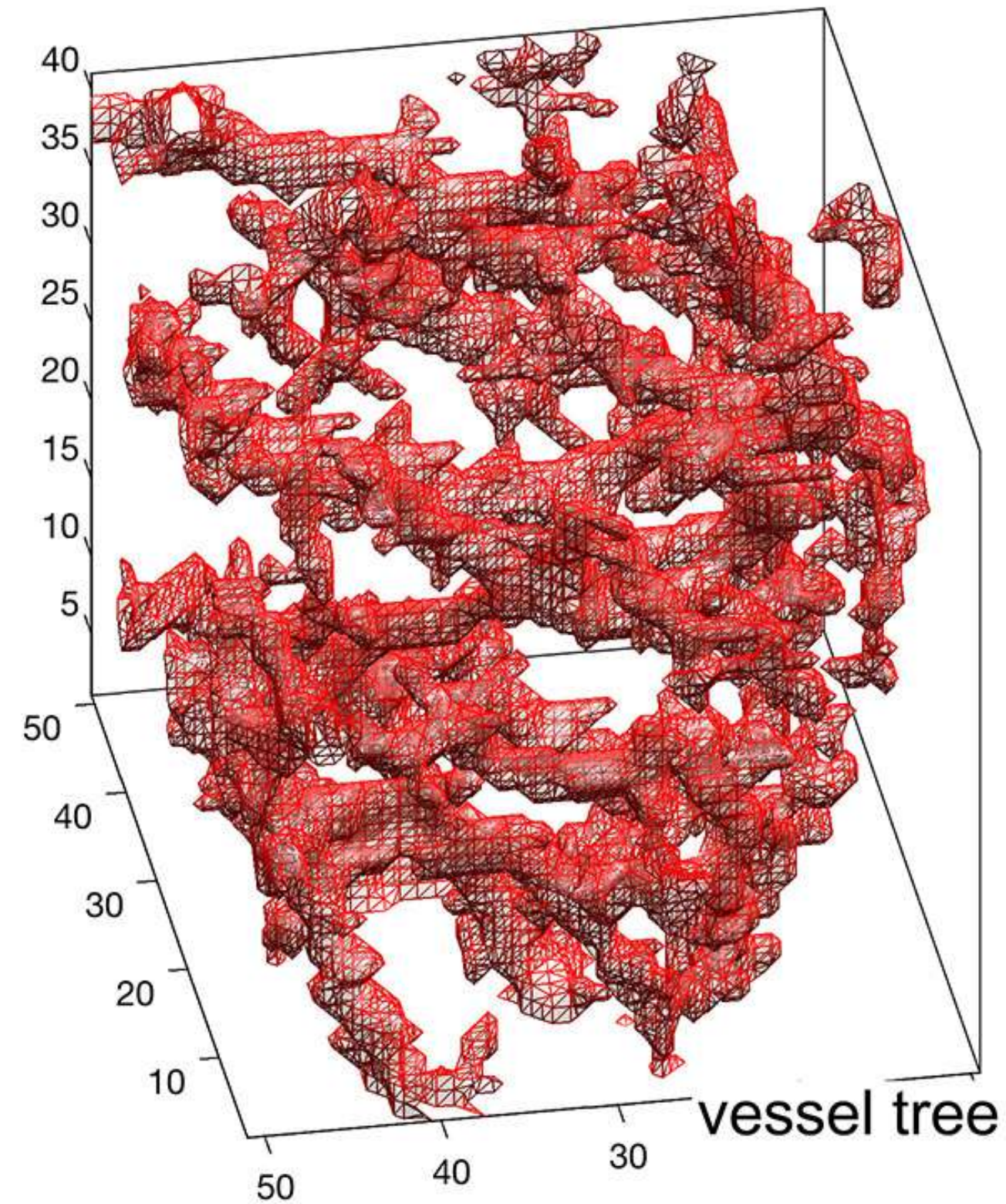
Statistically significant regions (F-stat) of mandible growth in age range between 0 and 20 years



Skeleton Representation of Lung Blood Vessel

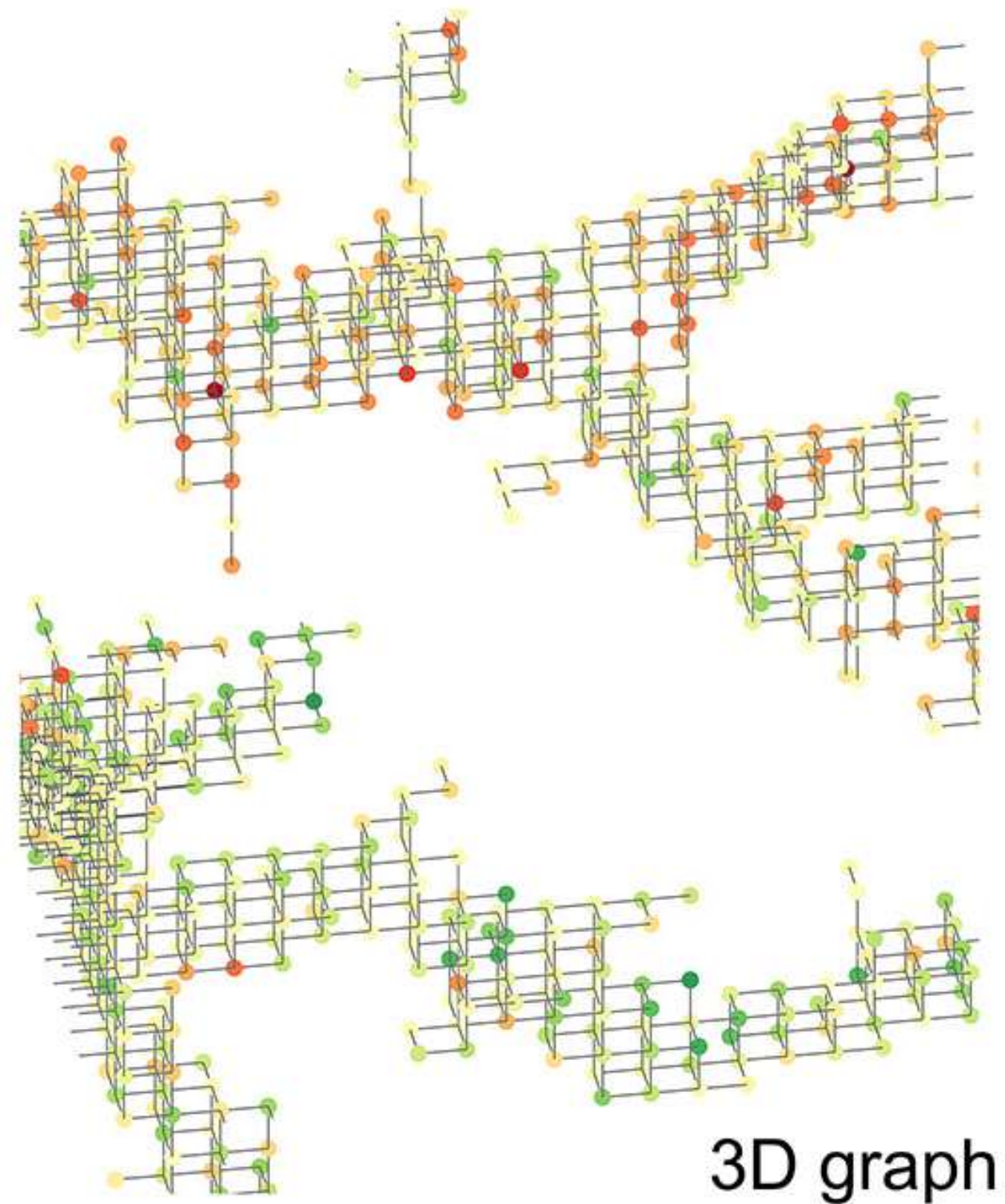
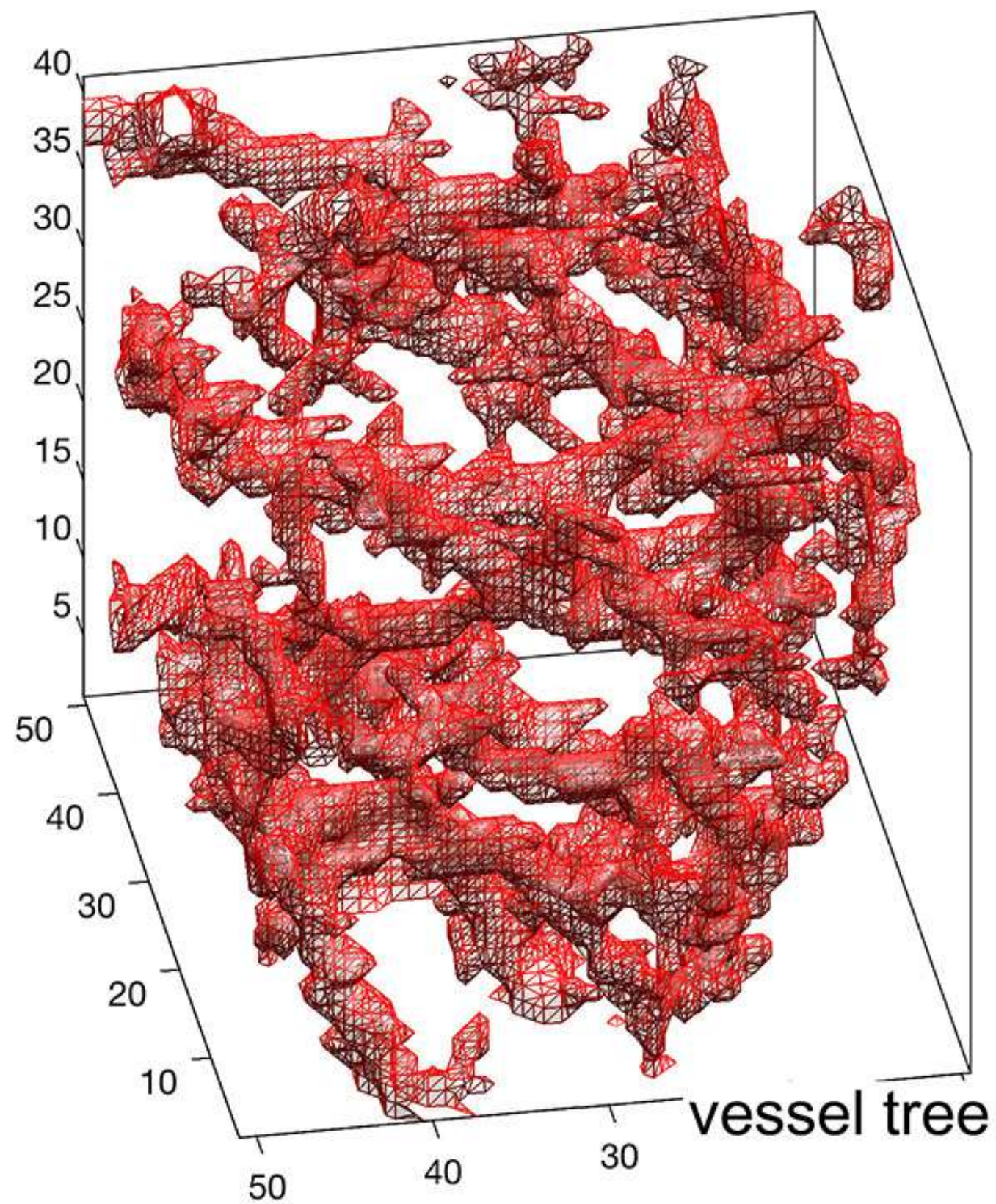
3D computed tomography

3D binary segmentation

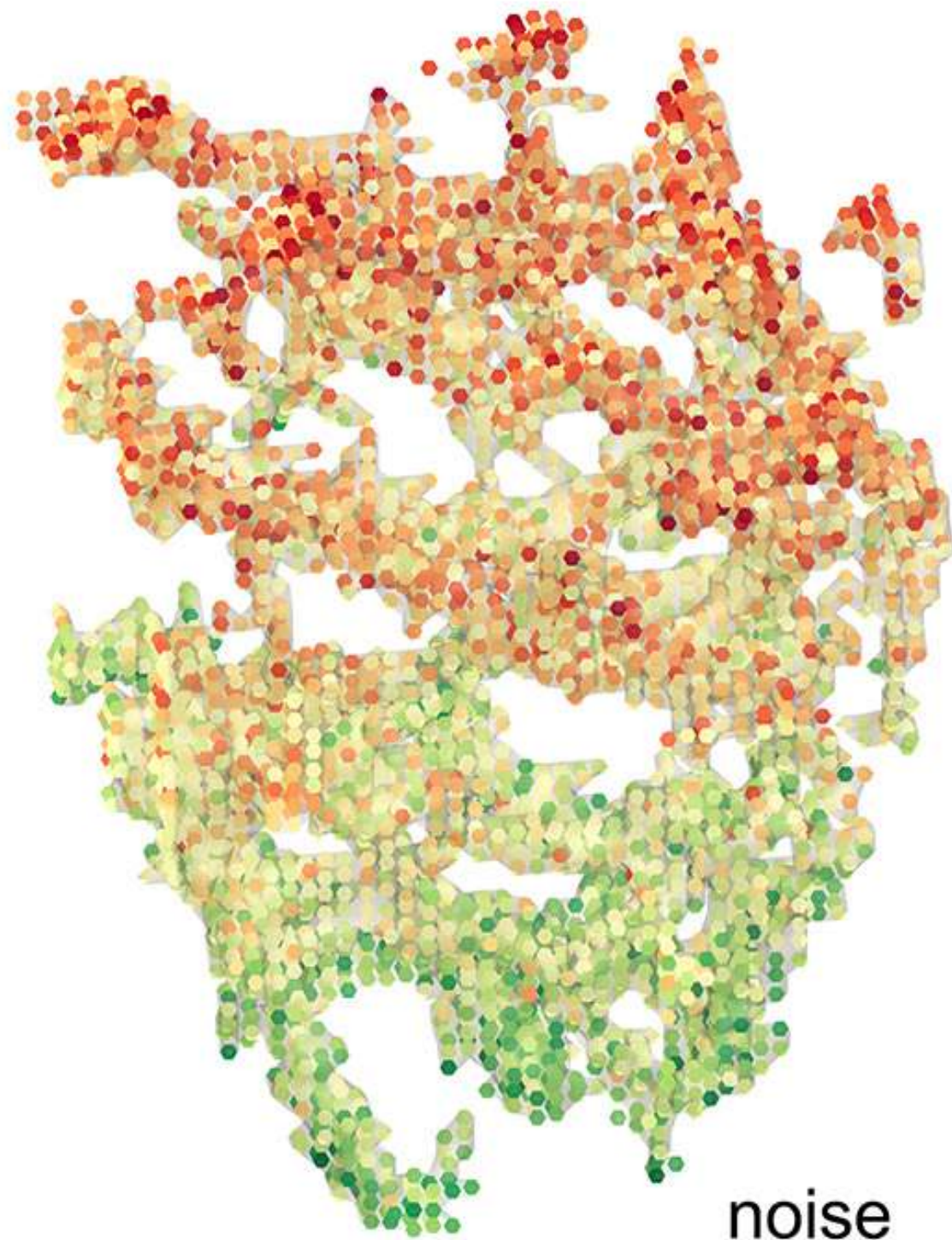


3D binary segmentation

3D graph using 6-neighbors

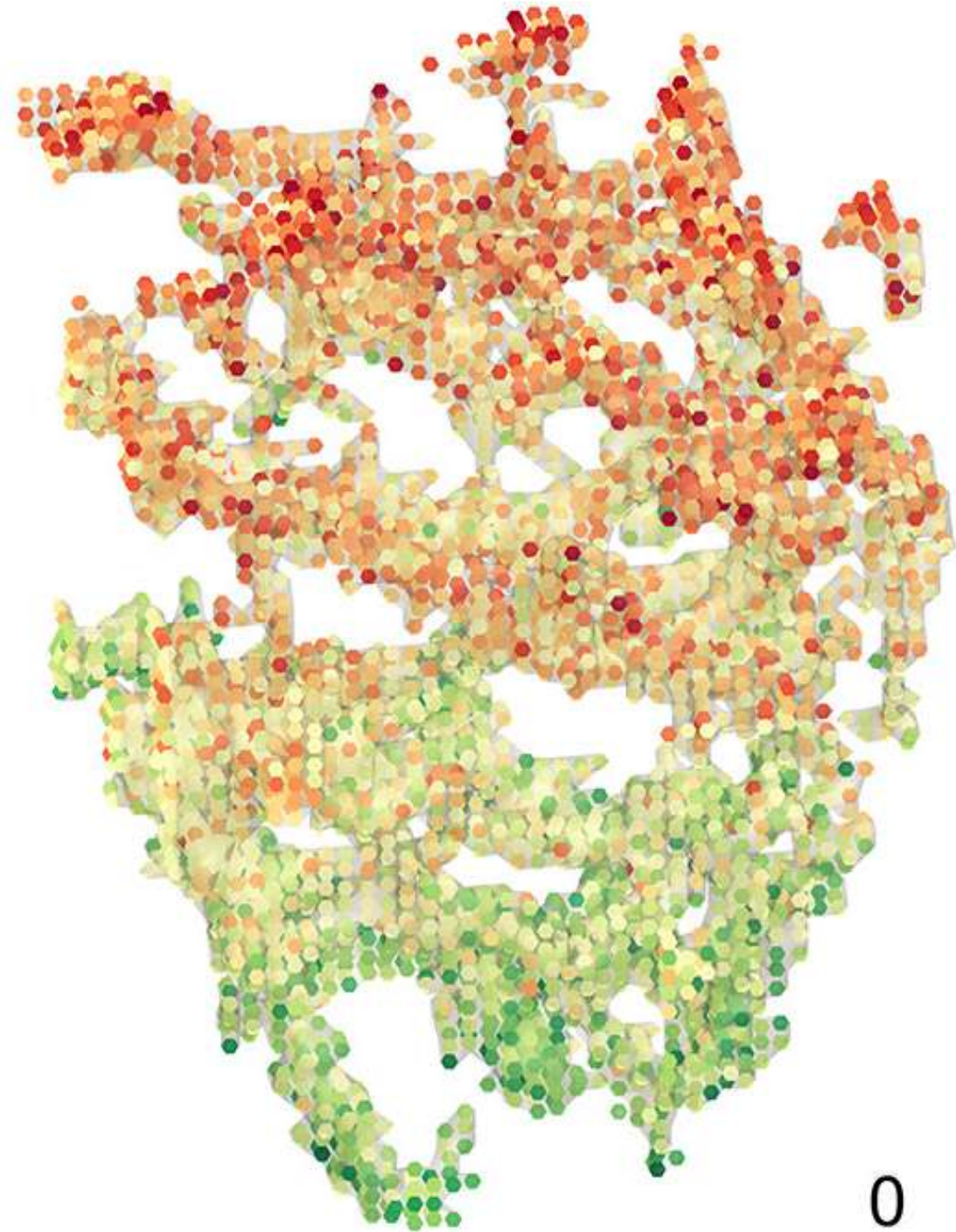


Z-coordinate
+ Gaussian noise



noise

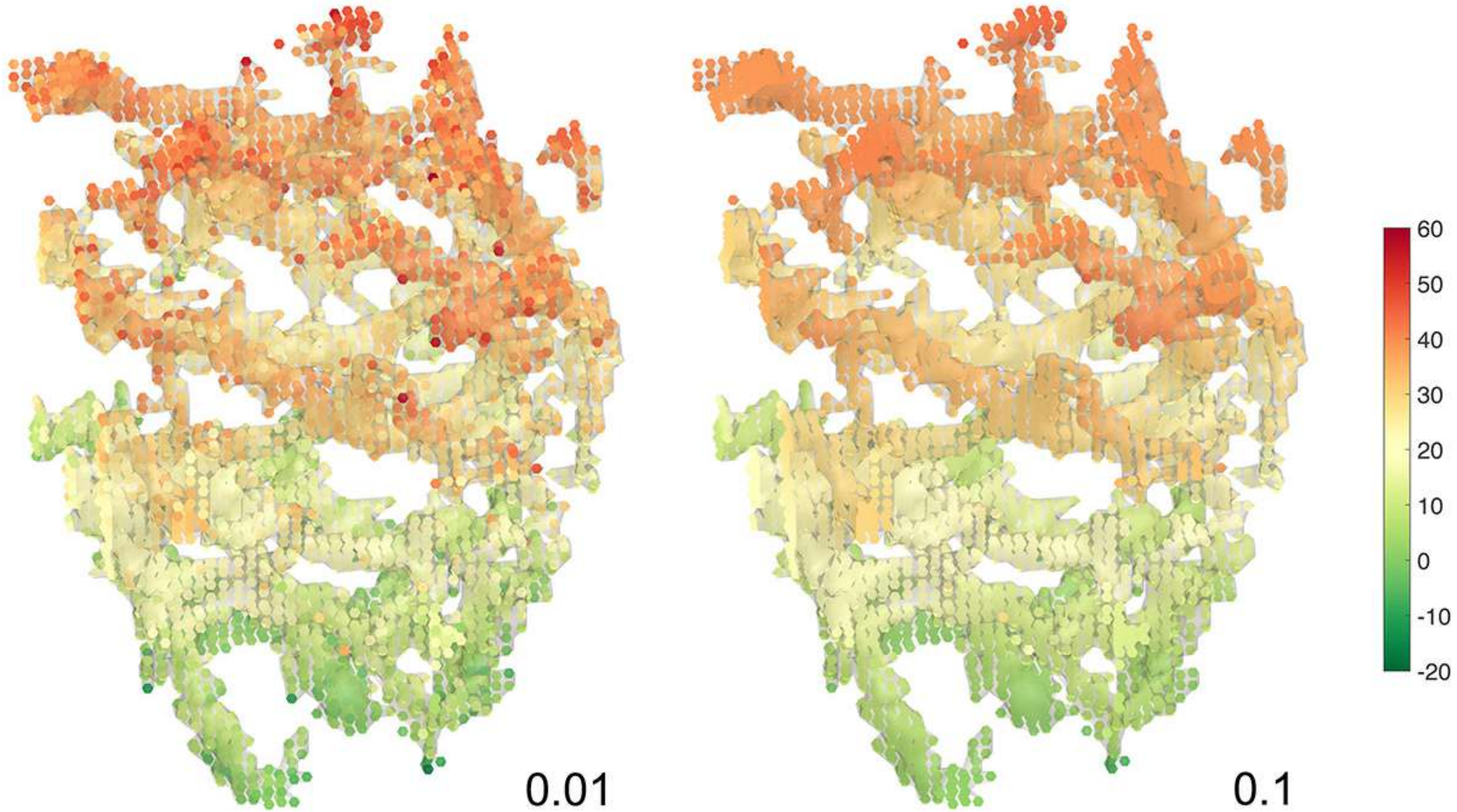
Fourier series expansion
with 6000 basis



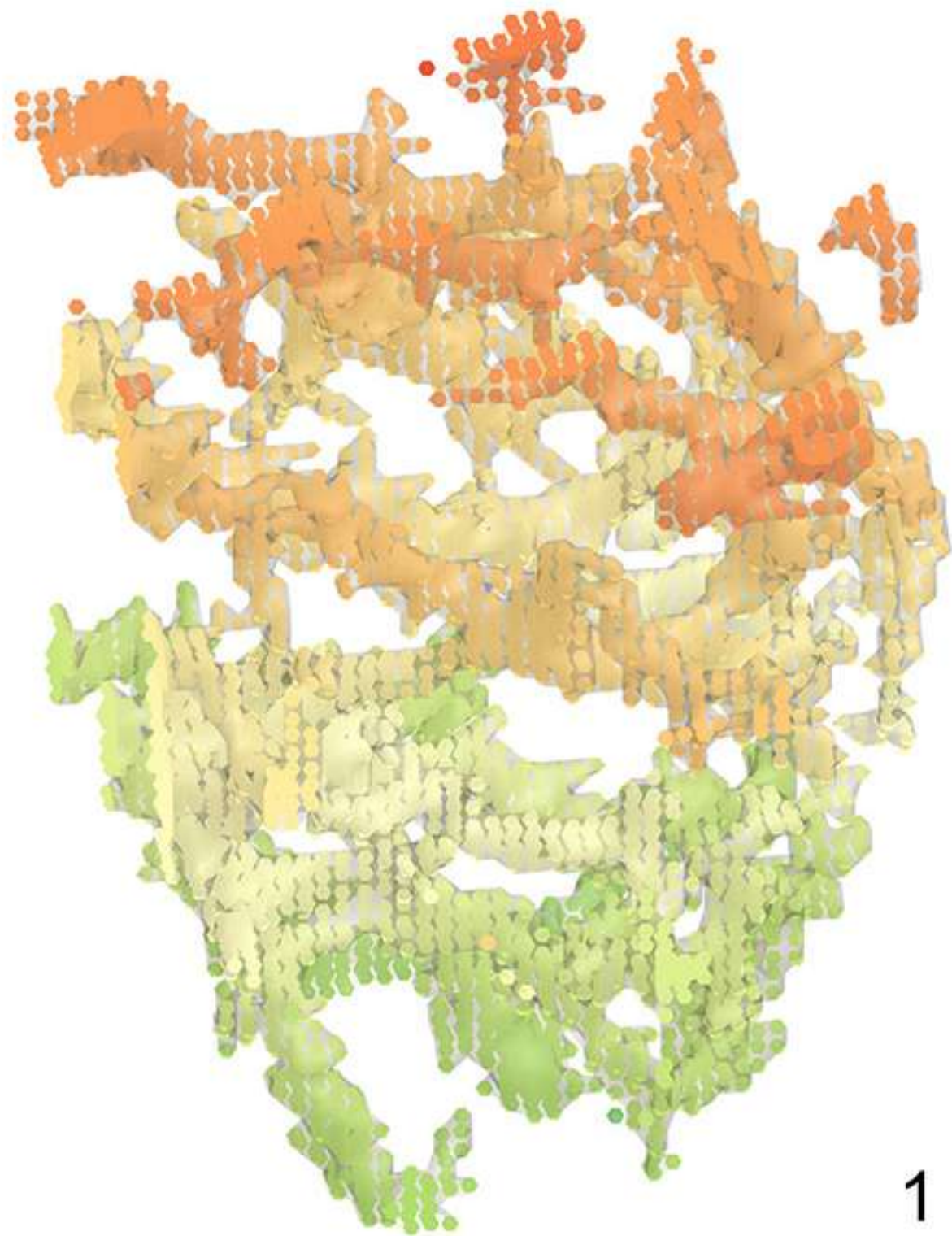
0



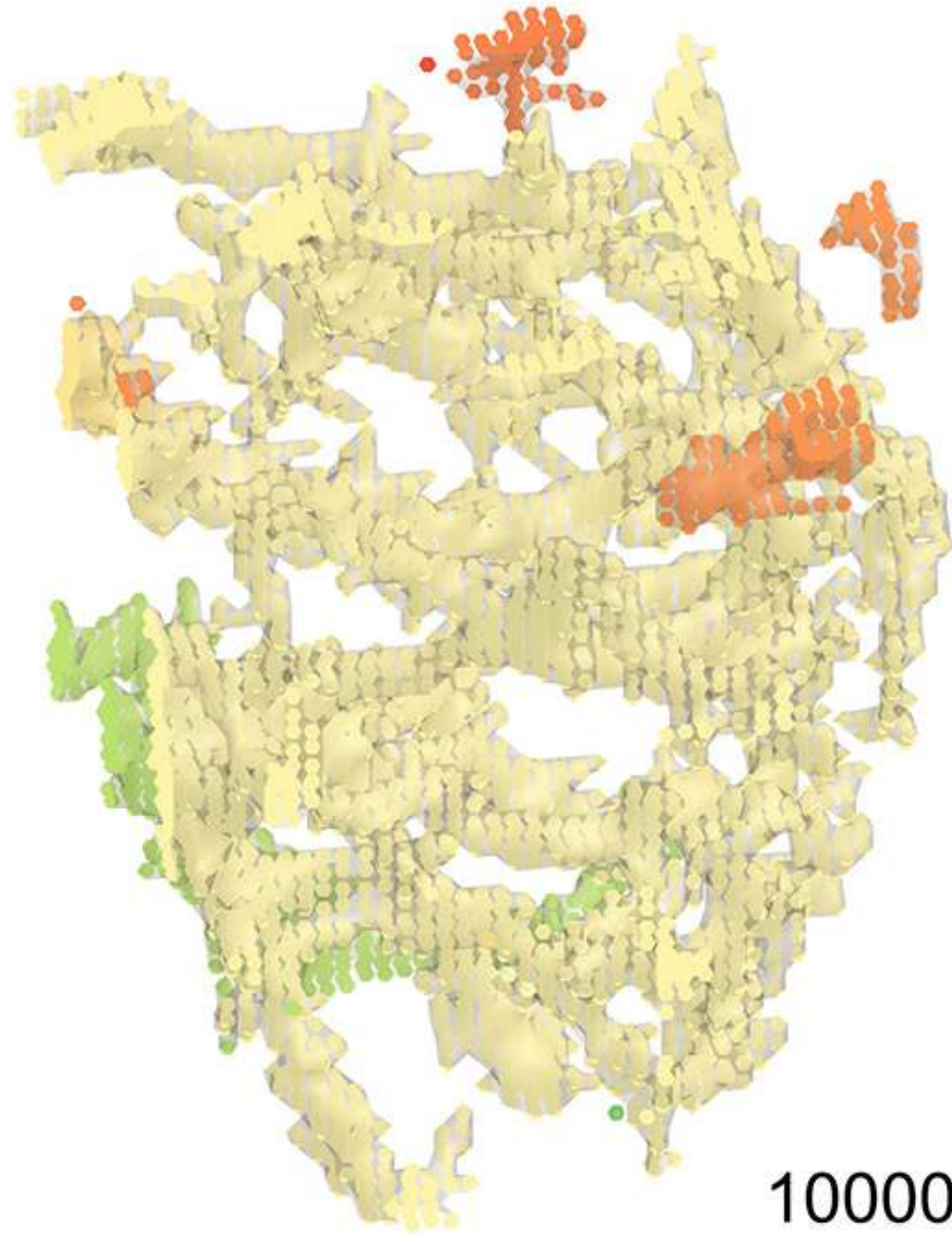
Heat kernel smoothing with 6000 basis



Heat kernel smoothing



1



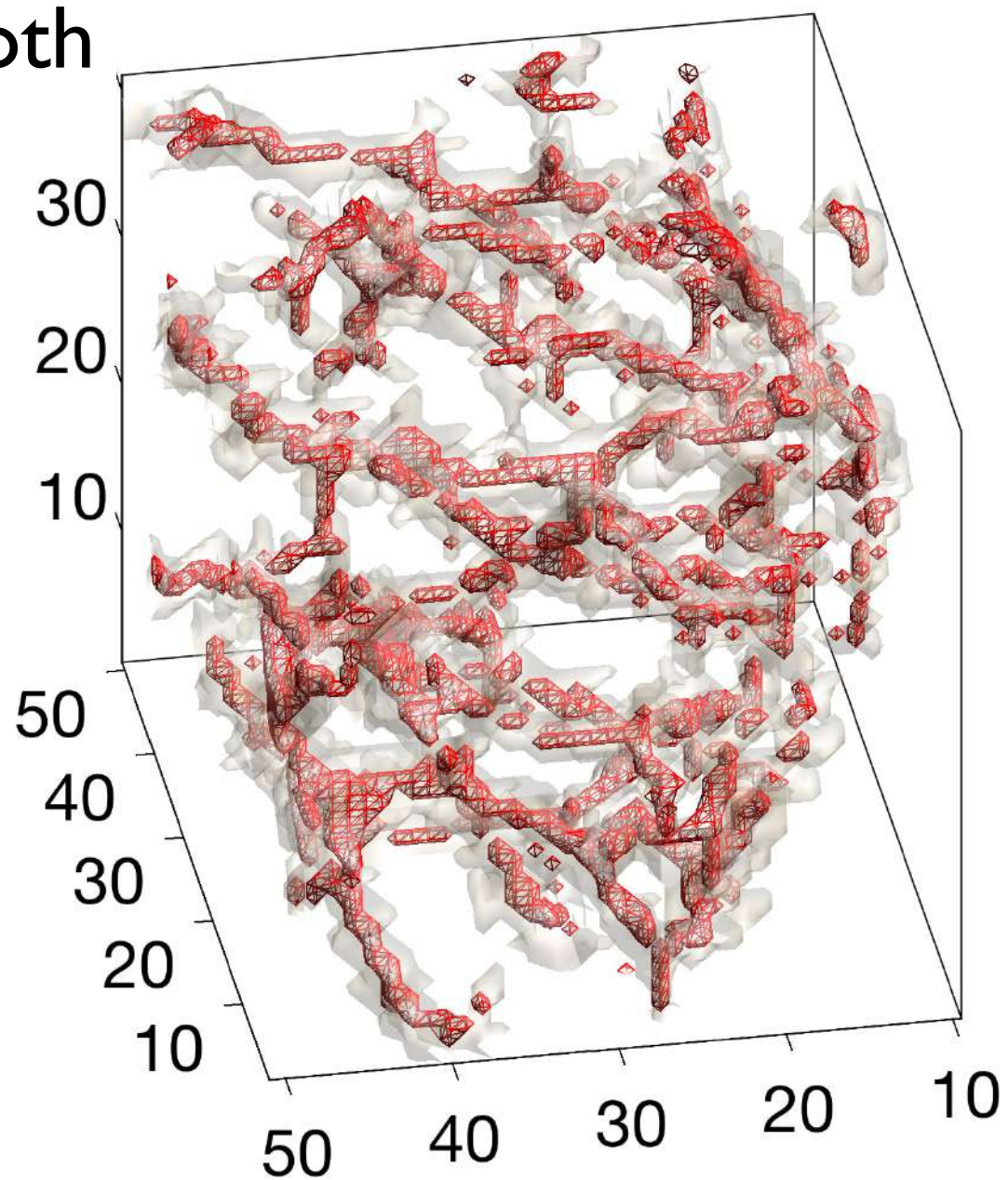
10000



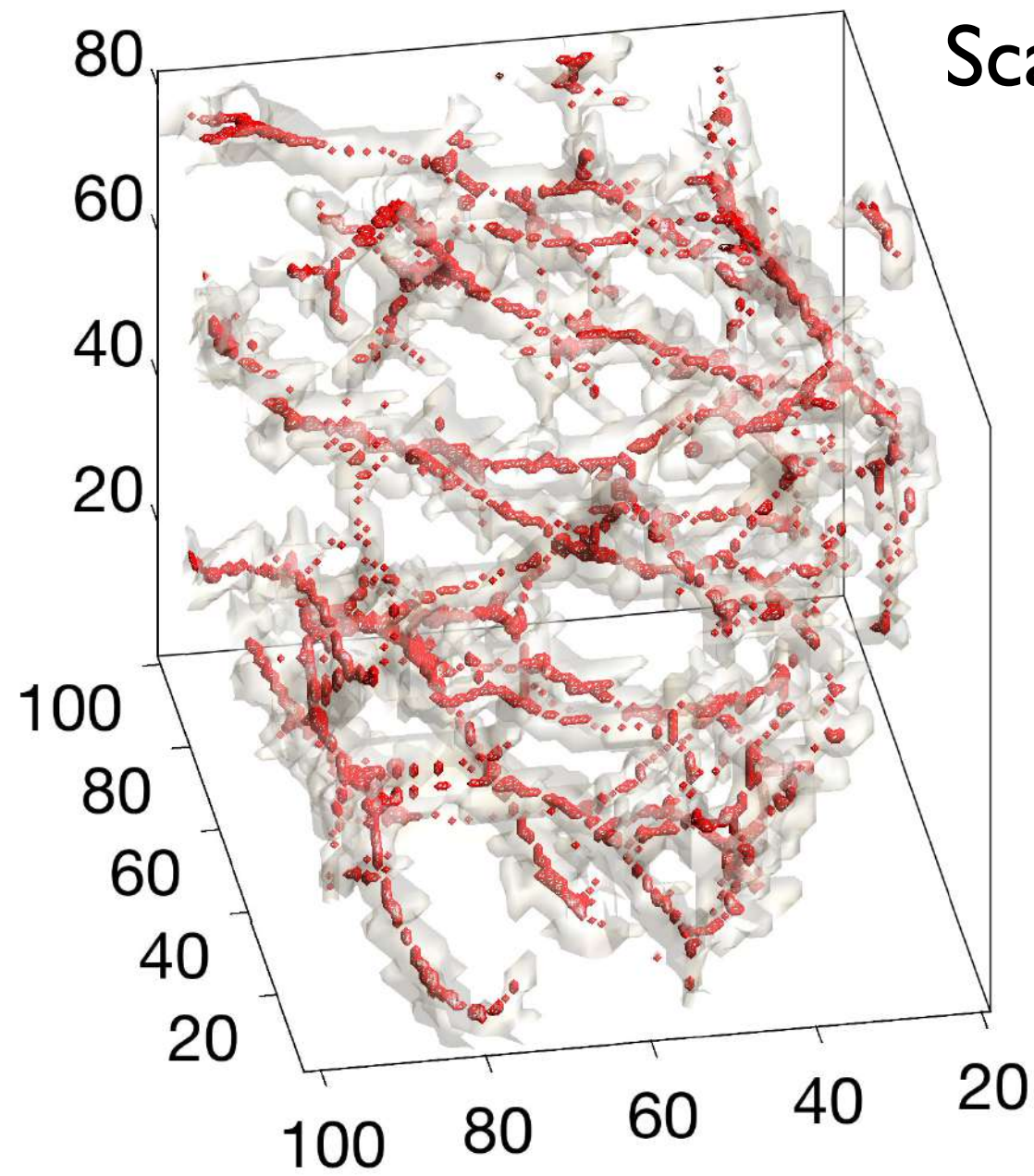
Skeleton representation of blood vessel



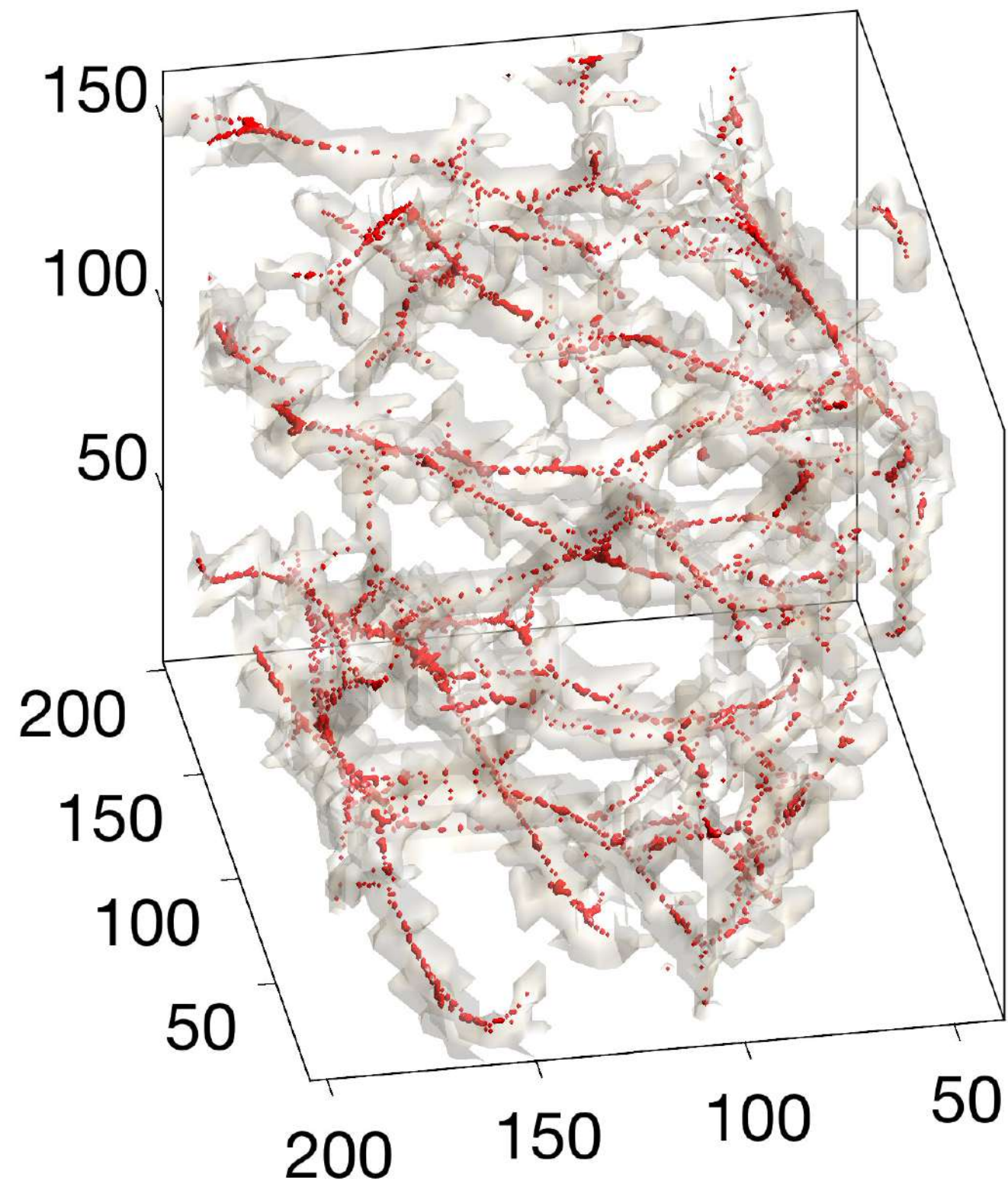
Smooth



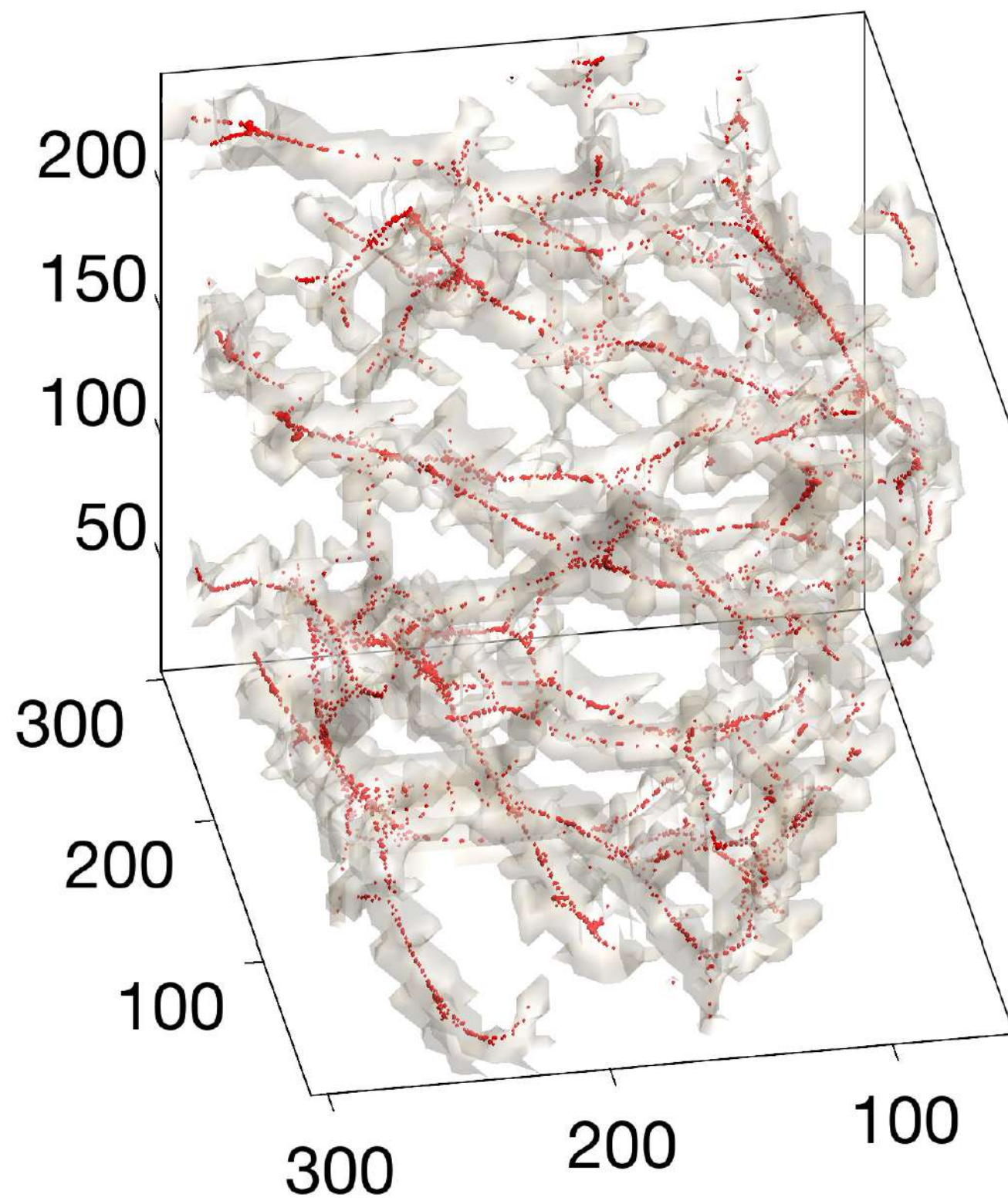
Scale up



Smooth + scale up



Smooth + scale up



Thank you



Any inquiry and collaboration request to
mkchung@wisc.edu